Hydrological Processes

WILEY

RESEARCH ARTICLE OPEN ACCESS

Global Comparison of Aqueous Geochemistry and Dissolved H_2/CH_4 in Continental Low Temperature Serpentinization–Influenced Environments

Alexandra May[1] | Ricardo Sánchez-Murillo[1] | Matthew O. Schrenk[2,3] | Esteban Gazel[4] | J. Maarten de Moor[5,6] | Christian Birkel[7,8] | Xiaoqiang Li[1] | Danelle Carr[1] | María Marta Chavarría[9]

[1]Department of Earth and Environmental Sciences, The University of Texas-Arlington, Arlington, Texas, USA | [2]Department of Microbiology, Genetics, and Immunology, Michigan State University, East Lansing, Michigan, USA | [3]Department of Earth and Environmental Sciences, Michigan State University, East Lansing, Michigan, USA | [4]Department of Earth and Atmospheric Sciences, Cornell University, Ithaca, New York, USA | [5]Observatorio Vulcanológico y Sismológico de Costa Rica, Universidad Nacional, Heredia, Costa Rica | [6]Department of Earth and Planetary Sciences, University of New Mexico, Albuquerque, New Mexico, USA | [7]Department of Geography and Water and Global Change Observatory, University of Costa Rica, San José, Costa Rica | [8]Leibniz Institute for Freshwater Ecology and Inland Fisheries, Berlin, Germany | [9]Programa de Investigación, Área de Conservación Guanacaste, Sistema Nacional de Areas de Conservación, Ministerio de Ambiente y Energía, Liberia, Costa Rica

Correspondence: Ricardo Sánchez-Murillo (ricardo.sanchezmurrillo@uta.edu)

Received: 25 September 2025 | **Revised:** 9 February 2026 | **Accepted:** 10 February 2026

Keywords: aqueous geochemistry | dissolved GeoH$_2$ and CH_4 | hyperalkaline fluids | regional hydrology | serpentinization-influenced environments

ABSTRACT

Since the 1960s, continental serpentinization-influenced environments have served as natural laboratories for investigating low-temperature aqueous geochemistry involving dissolved H_2 and CH_4, with broad implications for deep Earth elemental cycles, energy resources, and astrobiology. Here, we compiled, homogenised, and analysed geochemical data (aqueous and dissolved gas) from 34 studies focused exclusively on hyperalkaline spring seepage manifestations. The resulting database includes 2309 individual measurements spanning 16 physical and chemical variables. Tropical environments exhibited higher median values in Fe, Ni, CO_3^{2-}, dissolved inorganic carbon, and dissolved CH_4. Dissolved H_2 presented the highest median values in arid and cold continental settings. The arid environment also showed the highest median values in electrical conductivity (EC) and major ions (Na^+, K^+, Ca^{2+}, Cl^-). PCA dimension 1 (49.7%) was dominated by major ions, EC, Fe, Ni, CH_4, and H_2, reflecting strong controls on solute and redox-related chemistry, while Dimension 2 (8.7%) was primarily associated with water temperature. Tropical sites clustered toward Ni, Fe, oxidation–reduction potential, and Mg^{2+}, reflecting oxidising conditions and elevated metal concentrations, which are potentially derived from intense rock and soil monsoonal weathering. Arid sites trend toward OH^-, Cl^-, Ca^{2+}, Na^+, EC, and H_2, consistent with higher surface evaporative concentration and salinity in more evolved groundwater flows. Cold and temperate sites show greater variability, with hyperalkaline fluids tending toward higher pH and H_2. Our global comparison provides a systematic synthesis and framework for identifying both common patterns and site-specific differences in low-temperature continental serpentinization, underscoring the potential influence of regional hydrology, particularly groundwater flow and residence times, and water availability, in regulating conditions for H_2 and CH_4 production.

1 | Introduction

Serpentinization is a widespread process that involves the reaction of ultramafic rocks with fluids in environments such as mid-ocean ridges, forearc systems, subduction zones, and terrestrial ophiolites (Schrenk et al. 2013; Holm et al. 2015). This reaction results in the formation of serpentine group minerals (e.g., lizardite, chrysolite, antigorite) and secondary minerals such as brucite, and magnetite, along with a reduced hyperalkaline fluids enriched in hydrogen (hereafter $GeoH_2$) and methane (CH_4) (Coleman 1971; Frost and Beard 2007; Müntener 2010; Holm et al. 2015; Leong and Shock 2020). The degree of serpentinization refers to the extent to which the original ultramafic rock material has been altered into serpentine minerals, resulting in significant changes in physical properties (e.g., decrease in density ~3.2 to ~2.6 g/cm^3; volume increase by 35%–40%) (Hostetler et al. 1966; Thayer 1966; Park 1989), measured through various techniques such as mineralogical analysis, rock density measurements, and seismic velocity analysis (Miller and Christensen 1997; Chibati et al. 2022; Oufi et al. 2002; Reynard et al. 2007; Fujii et al. 2016).

Serpentinization is highly relevant to (i) understanding enigmatic prebiotic geochemical conditions, which may have supported the origin and early life evolution on Earth (Schulte et al. 2006), (ii) quantifying the deep carbon and other elemental cycles (Kelemen and Manning 2015), and (iii) developing sustainable energy technologies (Christiansen et al. 2024). This geological process plays a key role in a hypothesis suggesting that life may have originated in these environments, as this process produces $GeoH_2$ through the oxidation of ferrous (Fe^{2+}) to ferric (Fe^{3+}) iron, which can reduce CO_2 to CH_4 through the Sabatier reaction, mirroring the central biogeochemical process of methanogenesis (Neal and Stanger 1983; Seewald et al. 2006; Russell et al. 2010; Etiope 2017; Etiope and Sherwood Lollar 2013; McCollom and Seewald 2013; Preiner et al. 2018). Through the reduction of carbon sources via Fischer–Tropsch-type reactions (FTT), short-chain hydrocarbons, formate, acetate, and pyruvate can also be produced (Sleep et al. 2004; Etiope and Sherwood Lollar 2013; Holm et al. 2015; Etiope and Whiticar 2019; Leong and Shock 2020; Schwander et al. 2023). These are important for understanding the origins of life because they suggest pathways by which organic molecules could have formed on early Earth, and they pinpoint a particular geochemical environment in which the abiotic reduction of CO_2 is observed in nature (Russell et al. 2010). Furthermore, $GeoH_2$ is emerging as a clean and renewable energy source, potentially replacing oil and gas as a primary energy source if discovered in commercially viable reservoirs (Jackson et al. 2024). $GeoH_2$ production within the continental lithosphere has an estimated rate of ~10^{11} mol $GeoH_2$/year, which is comparable to that of oceanic lithospheric settings (Sherwood Lollar et al. 2014; Worman et al. 2016). Uncertainties in flux estimates stem from the complexities of serpentinization reactions, variations in the explored serpentinization sites, biological consumption, and the high reactivity and diffusivity of $GeoH_2$ (Worman et al. 2002, 2016; Ellis and Gelman 2024). Additionally, ultramafic rocks have been considered as hosts for CO_2 sequestration, as these rocks primarily consist of olivine and pyroxene that, when reacting with fluids, produce serpentine, magnetite, and stable carbonates (e.g., calcite, magnesite, and dolomite) (Kelemen et al. 2008).

Ophiolites represent tectonically emplaced fragments of oceanic lithosphere, including crustal and upper-mantle rocks, that record a range of formation environments and tectonic histories prior to continental exposure. While many well-preserved ophiolites are interpreted to have formed in supra-subduction zone settings, others reflect formation at mid-ocean ridges or plume-influenced environments, and many record hybrid or overprinted signatures (Miyashiro 1973; Coleman 1977; Gass 1980; Alabaster et al. 1982; Moores 1982; Pearce et al. 1984; Dick and Bullen 1984; Kelemen et al. 1995; Stern 2004; Dilek and Furnes 2011, 2014). In these ophiolitic settings, meteoric water interacts (via subsurface and surface water flow paths) with ultramafic rocks, providing natural testbed laboratories to study present-day, active serpentinization (e.g., Blank et al. 2009; Chavagnac et al. 2013; Szponar et al. 2013; Sánchez-Murillo et al. 2014; Cardace et al. 2015). Decades of research indicate that the availability of $GeoH_2$ and, indirectly, abiotic/biotic CH_4, is influenced by factors such as water-rock ratios, thermodynamic conditions such as temperature and pressure, catalyst-bearing minerals, and chemosynthetic microorganisms (Sleep et al. 2004; Song et al. 2021; McCollom and Bach 2009; Klein and Garrido 2011; Evans et al. 2013; Schrenk et al. 2013; Tiago and Veríssimo 2013; Foustoukos et al. 2015; Crespo-Medina et al. 2017; Neubeck et al. 2017; Barbier et al. 2020; Leong et al. 2023; Pappalardo et al. 2024). However, the role of regional hydrology and water availability (i.e., amount, water transit time, and recharge seasonality) in controlling $GeoH_2$/CH_4 generation, consumption, and carbon and other elemental cycling in serpentinised environments at the watershed scale remains less explored (Hrachowitz et al. 2016).

The hyperalkaline, reducing conditions generated by serpentinization create distinctive ecological niches that support diverse microbial communities, often invoked as analogs for early Earth and potential extraterrestrial life (Blank et al. 2009; McCollom and Seewald 2013; Schwander et al. 2023). The primary energy sources for chemosynthetic microorganisms in these environments include: H_2 oxidation, methanotrophy, methanogenesis, and sulphate reduction (McCollom and Seewald 2013). For instance, methanogenic Methanobacterium species have been reported in the Semail (Oman) and Santa Elena (Costa Rica) ophiolites, while Hydrogenophaga (H_2 oxidation) occurs in both sites as well as in the Massif du Sud (New Caledonia). Sulphate- and sulphur-reducing bacteria were found in the Massif du Sud, Semail, and CROMO wells in the Coast Range Ophiolite in California (Sánchez-Murillo et al. 2014; Crespo-Medina et al. 2014; Quéméneur et al. 2021, 2023; Rempfert et al. 2017; Fones et al. 2019; Nothaft et al. 2021; Templeton et al. 2021). In Santa Elena, methane-oxidising prokaryotes have also been detected (Sánchez-Murillo et al. 2014; Crespo-Medina et al. 2017), and methanogenic archaea comprise 40%–90% of archaeal sequences in hyperalkaline springs, likely reflecting elevated dissolved inorganic carbon (DIC; Crespo-Medina et al. 2017). At The Cedars (California) and Tablelands (Canada), Clostridia potentially contribute to localised H_2 production, accompanied by Betaproteobacteria mediating H_2 oxidation (Brazelton et al. 2012; Suzuki et al. 2013). The Chimaera seepage (Tekirova ophiolites, Turkey) hosts a broad metabolic repertoire involving CH_4, H_2, N_2, and Fe oxidation (Neubeck et al. 2017), whereas microbial diversity at Cabeço de Vide (Portugal) also points to CH_4-, H_2-, and sulfur-based metabolisms (Tiago and Veríssimo 2013).

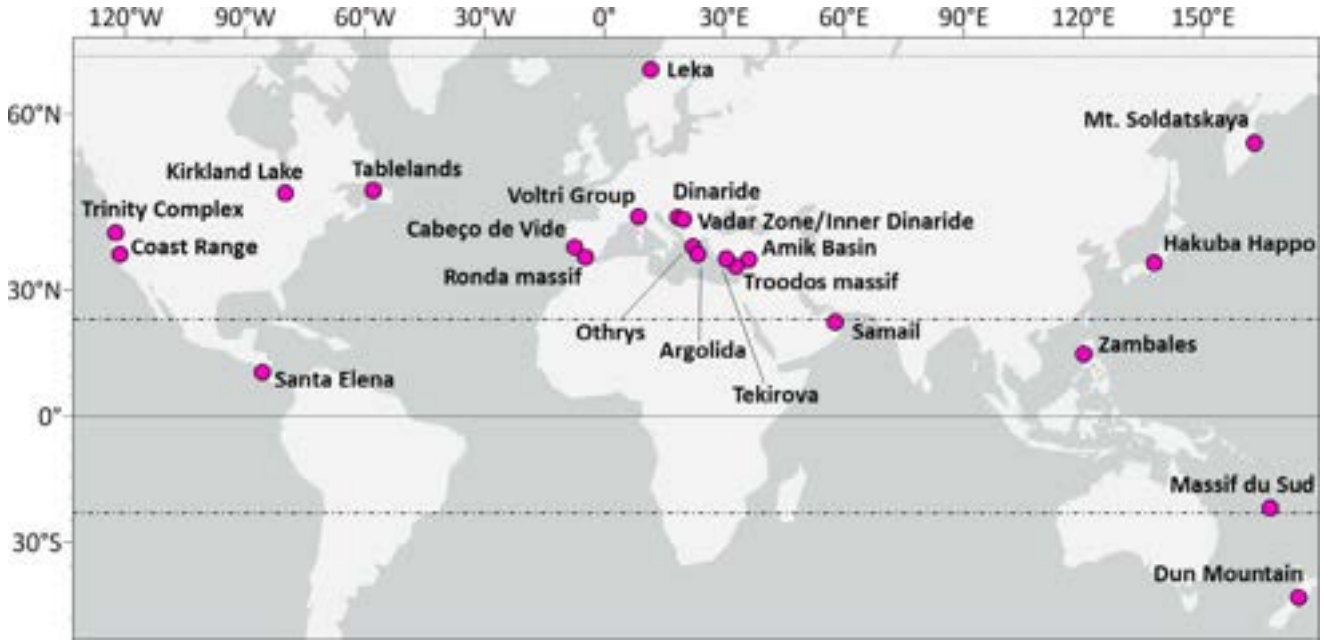

FIGURE 1 | Global continental serpentinization-influenced sites identified in the literature (1967–2025) (see Table 1 for site characteristics and references).

Interestingly, variations in fluid compositions due to mixing between hyperalkaline H_2-rich fluids and surrounding surface waters create a strong geochemical gradient that governs microbial distributions, as shown by Howells et al. (2022). Low-O_2 fluids favour H_2 oxidising taxa, whereas higher SO_4^{2-} concentrations promote sulfate reducers that preferentially utilise H_2 over methanogens, highlighting the role of fluid chemistry as a driver of microbial diversity in serpentinised systems (Howells et al. 2022).

2 | Type I and II Fluids in Continental Low Temperature Serpentinization

Numerous studies have been conducted to elucidate the principal processes of serpentinization occurring in low temperature continental systems that facilitate the formation of hyperalkaline fluids, along with associated $GeoH_2$, CH_4, microbial activity, other trace elements, and more complex compounds (surface fluid $<50°C$; e.g., Barnes et al. 1978; Leong and Shock 2020; Schrenk et al. 2013). Figure 1 and Table 1 highlight continental serpentinization-influenced sites (grouped by Köppen-Geiger climate regimes; Peel et al. 2007) in ophiolites and peridotite intrusions/massifs identified in the literature (1967–2025). These investigations also highlight the prevalent geochemical and physicochemical conditions in the hyperalkaline seepages, surrounding surface waters, and associated groundwater.

Meteoric water (precipitation) can react with ultramafic/mafic rocks through surface and subsurface flow paths (Figure 2). These reactions increase the dissolved Mg^{2+} and HCO_3^- contents, producing a moderately alkaline fluid of meteoric origin, which is the standard water type in the surface water streams (pH 7–9; Type I) (Leong and Shock 2020; Templeton et al. 2024). The Type I fluid can either discharge back to the surface through subsurface flow paths or percolate deeper, losing contact with the atmosphere and continuing to react with the ultramafic/mafic rocks, depending on the degree of fresh rock material (Figure 2). These reactions precipitate serpentine and other secondary minerals in the form of brucite, magnetite, and dolomite. During these reactions, Mg^{2+} and Ca^{2+} are released from the peridotite (e.g., olivine, orthopyroxene, clinopyroxene minerals) (Leong and Shock 2020). Mg^{2+} is incorporated into secondary minerals (likely reducing its concentration in the surface fluids), while Ca^{2+} accumulates in the serpentinising fluid due to the absence of a stable calcium mineral (Klein et al. 2014; Giampouras et al. 2019; Leong and Shock 2020). This loss of Ca^{2+} to the fluid phase is evident in the depletion of Ca^{2+} in serpentinised rocks and high concentration in the seepage fluids (Frost and Beard 2007). These water and rock reactions consume H^+ and release OH^-, which raises the pH, typically between 10 and 12 (Schwander et al. 2023).

The Type I fluid is transformed into a Ca^{2+}-OH^- rich fluid with high concentrations of dissolved $GeoH_2$ and CH_4 (pH up to~ 12; Type II) (Barnes et al. 1967; Templeton et al. 2024; Schrenk et al. 2013). At some continental serpentinising sites, the Type II fluids can have elevated K^+, Na^+, and Cl^- concentrations, which have been hypothesised to result from the leaching of sea salts introduced to the ophiolite during its emplacement, trapped paleo-seawater, contribution from fluids released by the subducting slab, as well as from the dissolution of minerals and/or sea spray (Neal and Stanger 1985; Peters 1993; Dewandel et al. 2005; Paukert et al. 2012; Sabuda et al. 2020; Evans et al. 2024). These ions can also be introduced from the interaction with paleo-seawater or leaching of fluid inclusions during serpentinization, and/or any rocks the fluids have previously interacted with along the groundwater flowlines (Boschetti and Toscani 2008; Chavagnac et al. 2013; Marques et al. 2018; Klein et al. 2019). Dissolved trace metals like Fe, Ni Co, Cu, and Cr are also frequently found in hyperalkaline fluids, as these are the most common metals in

TABLE 1 | Global continental serpentinization-influenced sites with available aqueous and gas geochemical data.

Country	Geologic setting	Köppen-Geiger climate	Climatology data	References
Costa Rica	Santa Elena Ophiolite	Tropical wet and dry (Aw)	Precipitation: Área de Conservación Guanacaste (Monthy: 2002–2024; annual sum: 1985–2024); Temperature: Villalobos and Retana 2000, Liberia Station (1957–1997)	Crespo-Medina et al. 2017; Sánchez-Murillo et al. 2014
New Caledonia	Massif du Sud	Tropical wet (Af)	Meteo France, Noumea Station (1991–2020) (Direction Interrégionale de Météo-France en Nouvelle-Calédonie et à Wallis-et-Futuna 2022)	Barnes et al. 1978; Cox et al. 1982; Deville and Prinzhofer 2016; Monnin et al. 2014, 2021; Ulrich et al. 2020
Philippines	Zambales Ophiolite/ Palawan Ophiolite	Tropical monsoon (Am)	Philippine Atmospheric, Geophysical and Astronomical Services Administration (PAGASA), Iba Station (1991–2020) (Republic of the Philippines, Department of Science and Technology, Philippine Atmospheric, Geophysical and Astronomical Services Administration, and Climatology and Agrometeorology Division. n.d.)	Abrajano et al. 1988; Abrajano et al. 1990; Cardace et al. 2015; Vacquand et al. 2018; Vergara et al. 2023; Wang et al. 2022; Meyer-Dombard et al. 2019; Aquino et al. 2025
Oman/UAE	Semail Ophiolite	Subtropical desert (BWh)	Directorate General of Meteorology, Ibra Station (1986–2009) (Directorate General of Meteorology 2020)	Barnes et al. 1978; Boulart et al. 2013; Chavagnac et al. 2013; Miller et al. 2016; Paukert et al. 2012; Neal and Stanger 1985; Etiope et al. 2015; Rempfert et al. 2017; Leong et al. 2023
Bosnia and Herzegovina	Dinaride Ophiolite	Oceanic (Cfb)	Federal Hydrometeorological Institute, Tuzla Station (1961–1990) (Federal Hydrometeorological Institute 2001–2024)	Etiope et al. 2017; Barnes et al. 1978
California, US	Coast Range/ Trinity Complex/Del Puerto Ophiolite	Mediterranean (Cs)	Western Regional Climate Center, Ukiah, CA Station (1893–2013) (Western Regional Climate Center 2016–2025)	Blank et al. 2009; Boschetti et al. 2017; Crespo-Medina et al. 2014; Suzuki et al. 2013
Cyprus	Troodos Massif	Mediterranean (Cs)	World Weather Information Service (Cyprus Meteorological Service), Prodromos Station (2002–2011)	Neal and Shand 2002
Greece	Argolida/Othrys ophiolites	Mediterranean (Cs)	World Weather Information Service (Hellenic National Meteorological Service), Larissa Station (Othrys), Tripolis Station (Argolida)	D'Alessandro et al. 2018; Etiope, Tsikouras, et al. 2013; Etiope, Vance, et al. 2013; Li Vigni et al. 2021
Italy	The Voltri Group Ophiolite Complex, Taro-Ceno Valley	Humid Subtropical (Cfa), Oceanic (Cfb)	World Weather Information Service (Italian Air Force-Department of Meteorology), Genova Station (1971–2000)	Boschetti and Toscani 2008; Boulart et al. 2013; Cipolli et al. 2004; Schwarzenbach et al. 2013

(Continues)

TABLE 1 | (Continued)

Country	Geologic setting	Köppen-Geiger climate	Climatology data	References
New Zealand	Dun Mountain Ophiolite	Oceanic (Cfb)	MetService, Nelson Airport Station	Pawson 2014
Portugal	Alter-do-Chão massif (Cabeço de Vide)	Mediterranean (Cs)	Instituto Portguês do Mar e da Atmosfera, Portalegre Station (1971–2000) (Instituto Português do Mar e da Atmosfera 2015)	Marques et al. 2008, 2018
Serbia	Dinaric and Vardar Zone ophiolite belts	Oceanic (Cfb)	Arsenović et al. 2015; Zlatibor Station (1961–2010)	Spahić et al. 2023
Spain	Ronda peridotite massif	Mediterranean (Cs)	World Weather Information Service (Agencia Estatal de Meteorologia), Malaga Station (1981–2010)	Etiope et al. 2016; Giampouras et al. 2019; Ojeda et al. 2023
Turkey	Tekirova Ophiolites, Amik Basin/The Kizildag Ophiolite Complex	Mediterranean (Cs)	World Weather Information Service (Turkish State Meteorological Service), Antalya Station (1929–2000; Tekoriva), Adana Station (1929–2000; Amik Basin)	D'Alessandro et al. 2018; Etiope et al. 2011; Meyer-Dombard et al. 2015; Hosgormez et al. 2008; Yuce et al. 2014
Japan	Hakuba Happo hot springs	Humid subtropical (Cfa)	—	Suda et al. 2014, 2022
Canada	Tablelands massif; Kirkland Lake kimberlite field	Humid continental (Df)	Government of Newfoundland and Labrador, Cow Head Station (1983–2018) (Government of Newfoundland and Labrador. n.d.)	Brazelton et al. 2012; Cook et al. 2021; Cumming et al. 2019; Szponar et al. 2013; Sader et al. 2007
Norway	Leka Ophiolite Complex	Subarctic (Dw)	—	Okland et al. 2012; Iyer et al. 2008
Russia	Mt. Soldatsky massif	Subarctic (Dw)	World Weather Information Service (Russian Federal Service for Hydrometeorology and Environmental Monitoring), Petropavlovsk-Kamchatsky Station	Taran et al. 2023, 2024

ultramafic rocks (Schwander et al. 2023). Another common characteristic of hyperalkaline fluids is low concentrations of dissolved CO_2 because the dominant form of carbonate when pH > 8.3 is CO_3^{2-}, which readily precipitates in the presence of divalent cations at high pH (Leong and Shock 2020). The Type II fluids can emerge as hyperalkaline seepages through structures such as faults, peridotite/dikes contact areas, or fractures (Figure 2).

The hyperalkaline fluid interacts with atmospheric CO_2, precipitating calcium carbonate, also known as travertine deposits, which can be seen as terrace deposits in former and current flow paths of the hyperalkaline fluids (Figure 2; Barnes et al. 1978; Schrenk et al. 2013). Another notable feature is a thin crystalline carbonate crust that forms a film on the surface of the hyperalkaline fluids (Figure 2). Gas bubbles can be trapped depending on the thickness of the carbonate crust (Figure 2). The mixing between Type II fluid and Type I fluid generates a third fluid type (Type III) (not shown in Figure 2), precipitating Ca-rich carbonates and brucite. This process reduces the fluid pH to a moderately alkaline level with a more varied redox potential and dissolved species depending on the degree of mixing (Paukert et al. 2012; Leong and Shock 2020). A recent study by Leong et al. (2021) in the Semail Ophiolite in Oman classified a fourth fluid type with compositions intermediate between Type I and Type II (pH 9–11; low dissolved Si content; Type IV). This fluid is not a product of mixing but instead represents a transitional stage between Type I and Type II (not shown in Figure 2).

3 | Methodology

3.1 | Climate Data

Monthly precipitation and temperature data for each continental serpentinization-influenced site were compiled from national meteorological agencies or published literature, as listed in Table 1 (WMO 2024; World Bank Group 2025; Table S1). Climate stations were selected based on geographical proximity and prevalence of long-term data records (> 10 years). For the sites in Costa Rica, Cyprus, Italy, Oman, the United States, Russia, Greece, Spain, Turkey, and New Zealand, only the maximum and minimum monthly temperatures were compiled; therefore, average monthly temperatures were calculated as the mean of these values. For the site in Canada, monthly precipitation and average temperature data were obtained from 1983 to 2018; therefore, values were averaged for each month across all years to obtain the mean monthly precipitation and temperature. Lastly, the monthly precipitation data (2002–2024) for the site in Costa Rica were provided by the Área de Conservación Guanacaste and used to calculate average monthly values. Mean annual precipitation (MAP) for each site was calculated by summing the average monthly precipitation totals. For the site in Costa Rica, the MAP was calculated by averaging yearly precipitation amounts from 1985 to 2024. Subsequently, each site was categorised according to the Köppen-Geiger climate classification (i.e., tropical, temperate, arid, and cold continental) (Peel et al. 2007). To visualise seasonal trends, climographs depicting average monthly temperature and precipitation were generated.

3.2 | Geochemical Data

A geochemical data compilation, cleaning, and organisation process was conducted to address the lack of comparative statistical analyses in existing studies on low temperature serpentinization in ophiolitic settings with available geochemical data for hyperalkaline seepages. Geochemical data from 34 studies were reviewed, homogenised, and compiled, resulting in the extraction of 2309 individual data points across 16 relevant physical and chemical variables. To highlight the lack of consistent sampling, 322 hyperalkaline samples from four climate regimes were compared. Among these, the most frequently reported variables include pH, seepage fluid temperature, Ca^{2+}, Na^+, Cl^-, and Mg^{2+}, while others are underreported (Ni, Fe, DIC, alkalinity, CH_4, H_2; Figure S1 and Table S2). These data were compiled into a centralised database and standardised by converting all measurements to consistent units for statistical comparison. Supporting Information is also available at CUAHSI HydroShare repository: http://www.hydroshare.org/resource/9ad700ebb18947e3a49662d78dfaa21b.

Paired dissolved CH_4 and $\delta^{13}C$-CH_4 data in serpentinising fluids were compiled from previously published studies. Site locations and corresponding references include Argolida (D'Alessandro et al. 2018), Cabeço de Vide (Marques et al. 2018), Coast Range (Cook et al. 2021), Dinaride (Etiope et al. 2017), Dun Mountain (Pawson 2014), Zambales (Crespo-Medina et al. 2017), Santa Elena (Crespo-Medina et al. 2017), Orthrys (Etiope, Tsikouras, et al. 2013; Etiope, Vance, et al. 2013), Ronda massif (Etiope et al. 2016), Semail (Miller et al. 2016), Tablelands (Szponar et al. 2013; Cumming et al. 2019). To differentiate between H_2 and CH_4-dominant systems, the ratio (log-scaled) between H_2/CH_4 [–, dimensionless] was calculated only using samples collected at the same time in a single location, following Boulart et al. (2013). Data sources include tropical (Cardace et al. 2015; Crespo-Medina et al. 2017; Unpublished data), continental (Szponar et al. 2013; Morrill et al. 2014; Cumming et al. 2019), arid (Boulart et al. 2013; Miller et al. 2016; Rempfert et al. 2017), and temperate systems (Boulart et al. 2013; Etiope, Tsikouras, et al. 2013; Etiope, Vance, et al. 2013; Etiope et al. 2016, 2017; Li Vigni et al. 2021; Ojeda et al. 2023).

3.3 | Recent Tropical Geochemical Data

To complement the tropical geochemical data, information from recent sampling campaigns in the Santa Elena Ophiolite (Costa Rica) was included. Four field campaigns were conducted during January 2024, May 2024, December 2024, and March 2025. A set of parameters, including water temperature (°C), pH, EC (mS/cm), and ORP (mV), were measured in situ using portable probes (Oakton Environmental Express Model 35 660-76 and Bante Instruments Model 902P). For pH, three-point calibrations were conducted using Biopharm Buffer Reference Solution at 4.00 ± 0.01, 7.00 ± 0.01, and 10.00 ± 0.02 at 25°C. For EC, Oakton Conductivity Standards of 84 and 1413 µS/cm were used.

Major cations, anions, and DIC were analysed at the Chemistry School of Univesidad Nacional (Heredia, Costa Rica). For major cation and anion analysis, hyperalkaline fluids were sampled directly from seepages, filtered using a 0.45 mm PTFE filter, and

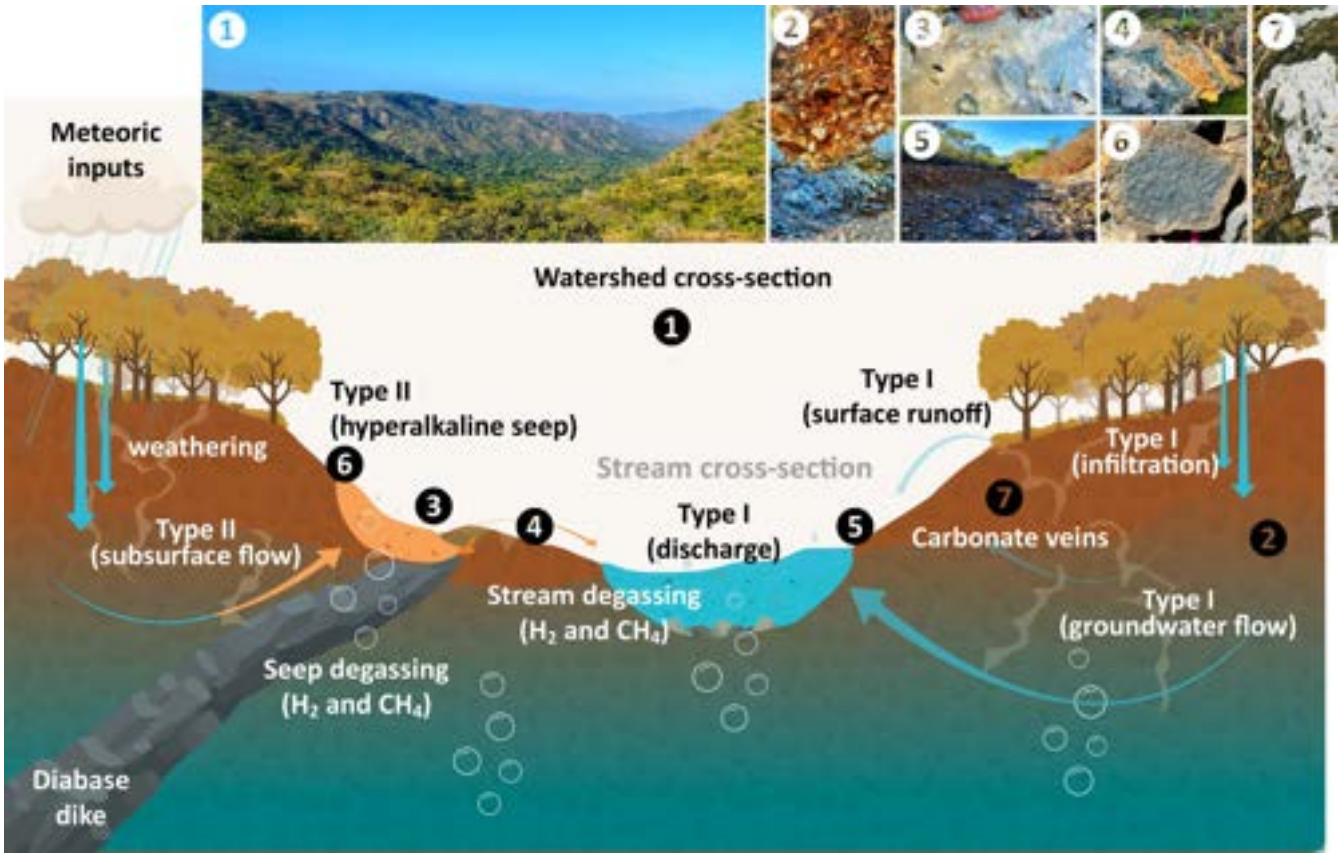

FIGURE 2 | Conceptual diagram showing hydrological and geochemical processes within the Santa Elena Ophiolite in northwestern Costa Rica: (1) Potrero Grande watershed cross section overview; (2) rock weathering and soil genesis profile (Murciélago watershed); (3) hyperalkaline (Type II water) hosting environment (pH > 11.6) (Danta watershed). Atmospheric carbon dioxide is immediately sequestrated and results in a surface white calcite layer. Below this layer, gas bubbles from the serpentinization reaction (mainly H_2 and CH_4) are trapped; (4) hyperalkaline seepage (Type II water) into a surface water body (Type I water) (Danta watershed), showing peridotite (in dark), red-orange travertine deposits, and calcite precipitation (white crust); (5) excavated non-perennial stream cross-section after the impact of a tropical storm (Murciélago watershed), photo reflecting baseflow conditions; (6) weathered versus fresh peridotite rock (Calera watershed); (7) carbonate vein deposits (Potrero Grande watershed). Photo Credits: Ricardo Sánchez-Murillo.

transferred into 5 mL sterile PP vials. Samples were preserved until analysis at 5°C (between 1 and 2 weeks after collection). Major cations and anions were analysed using ion chromatography (Thermo Scientific ICS-5000+, CA, USA) following Method 4110 (American Public Health Association et al. 2024). Blanks and recovery standards were also included in each batch of samples to ensure the quality of the analysis. Samples with a charge-balance error > 10% were not included in the final dataset. Calibration and recovery standards were prepared using NIST traceable standards (TraceCERT, Merck KGaA, Darmstadt, Germany). For DIC analysis, fluids were sampled into 250 mL amber bottles with no headspace and stored under dark conditions at 5°C until analysis (typically 1 week after collection). DIC contents wereermined using a total carbon analyser (Aurora 1030W, OI Analytical) following the Heated-Persulfate Oxidation Method 5310C (American Public Health Association et al. 2024). Each water sample was filtered using 0.45 μm PTFE filter into 100 mL pre-cleaned vials. A standard curve was conducted using six calibration solutions (i.e., stock solution of anhydrous primary-standard-grade potassium biphthalate, $C_8H_5KO_4$) (Method 5310 C; American Public Health Association et al. 2024). The quantification and detection limits were 0.05 and 0.03 mg C L^{-1} (Sánchez-Murillo et al. 2019, 2022). DIC was finally calculated as the difference between total carbon and total organic carbon.

Samples for the determination of heavy and alkaline metals were treated with nitric acid in the field to prevent precipitation. Samples collected in January 2024 and May 2024 were analysed by the Laboratorio de Análisis Ambiental, Universidad Nacional (Heredia, Costa Rica), following the methods outlined in Standard Methods 3125 A and B and 3030 A and B (American Public Health Association et al. 2024). Water samples collected in December 2024 and March 2025 were analysed by the Shimadzu Center for Environmental Forensics and Material Science at The University of Texas at Arlington. For ICP-MS analysis (ICPMS-2030), all the water samples were filtered through a PTFE-L 0.45 μm syringe filter (Thermo Scientific Titan3). Samples were run at both 2× and 10× dilutions using a 2% nitric acid solution (LCMS grade water, trace metal grade nitric acid). The blank was also prepared at 2× and 10× dilutions and was subtracted from the corresponding sample data. For alkalinity analysis, bottles were filled with no headspace and sealed with parafilm to prevent CO_2 exchange. Expanded alkalinity was analysed by potentiometric titration using a Hach Digital Titrator Model 16 900 (Standard Method 2320b). Titration

accuracy was ±1% for titrations exceeding 100 digits and ±1 digit for titrations below 100 digits. Results from phenolphthalein and total alkalinity measurements allowed for the stoichiometric determination of bicarbonate, carbonate, and hydroxide, with concentrations reported in mg/L as $CaCO_3$ equivalents.

For dissolved H_2 and CH_4 sample collection, Giggenbach bottles (Adams & Chittenden Scientific Glass Coop; 200 mL) were prepared with 50 mL of 4 N NaOH, and a vacuum was applied to avoid gas presence (Giggenbach 1975). The bottles were weighed before and after sampling with a precision of 0.1 g. During field sampling, the bottles were filled to two-thirds capacity, leaving a headspace of 70–90 mL to capture gases exsolved from the water for analysis. Samples were analysed by gas chromatography in the Geochemistry Laboratory at OVSICORI (National University, Heredia, Costa Rica) using the methods described in detail by de Moor et al. (2025).

3.4 | Statistical Data Treatment

3.4.1 | Pairwise Comparisons

Box plots were generated for the selected 16 variables to visualise the distribution and variability across the different global sites grouped by their Köppen-Geiger climate classification. For improved clarity and interpretability of the box plots, specific outlier values were excluded from the data visualisation. Specifically, extremely high electrical conductivity (EC) values reported by Crespo-Medina et al. (2014) for CROMO wells (8200 and 11 200 µS/cm) were removed. Additionally, K^+ concentrations from Cook et al. (2021) were excluded for the Cedars site (Grotto Pool Spring and Barns Spring Complex; 159.00 and 30.70 mmol/L), as well as the Tablelands site (WHC2; 20.20 mmol/L). These exclusions were made solely for visualisation purposes and did not affect any statistical analyses or interpretations derived from the full dataset. Using the Wilcoxon sum-rank test ($\alpha = 0.05$), we conducted a statistical comparison of pH, EC, oxidation–reduction potential (ORP), major ion compositions, trace elements, DIC (reported as total inorganic carbon for Tablelands; TIC), and dissolved $GeoH_2$/CH_4 concentrations across hyperalkaline seepages at continental serpentinising sites (Table S3). The following sites were excluded from the statistical comparisons: the Leka Ophiolite in Norway, which includes only geobiology and groundwater/surface water data; the Hakuba Happo hot springs in Japan; Kirkland Lake in Canada, a kimberlite field; and the Trinity Complex (Aqua de Ney), noted for its discharge of saline hyperalkaline fluid in a continental environment (Monnin et al. 2021).

3.4.2 | Principal Component Analysis

To address missing values in the geochemical dataset, we applied a regularised iterative principal component analysis (PCA) imputation using the missMDA package in R (Josse and Husson 2016). Numerical variables were extracted and standardised, while categorical descriptors (e.g., *Climate* regimes) were excluded from the imputation but later incorporated as supplementary factors for visualisation. The optimal number of components for imputation was determined via cross-validation with the estim_ncpPCA function, minimising reconstruction error across candidate dimensions. Missing values were then estimated with the imputePCA algorithm, which iteratively reconstructs the data matrix from a low-rank PCA model while applying regularisation to prevent overfitting. The completed dataset was subsequently analysed with PCA (FactoMineR) (Lê et al. 2008), using unit variance scaling to ensure comparability across variables, and the *Climate* factor was used post hoc to aid in the interpretation of group structure in the multivariate space.

4 | Results

4.1 | Hydroclimatic Generalities

Figure 3 depicts climographs showing long-term monthly precipitation and atmospheric temperature across the sites grouped by the main climate groups: arid, tropical, temperate, and cold continental. In temperate and cold continental environments, precipitation mostly consists of seasonal snow/rainfall events, in most cases resulting in slow and old regional groundwater circulation. In arid and semi-arid areas, annual precipitation is low, and large evaporative losses under low relative humidity often limit infiltration and increase solute concentrations via evapoconcentration. Contrary to these scenarios, in tropical settings (e.g., Santa Elena, Costa Rica; Zambales, Philippines; and Le Crouen, New Caledonia) (Sánchez-Murillo et al. 2014; Ulrich et al. 2020; Wang et al. 2022), rainfall amount and intensity are usually greater and occur throughout several monsoonal months (Figure 3), facilitating infiltration and deep percolation (i.e., naturally stimulated recharge). For example, the annual precipitation in Costa Rica is 14× greater than in the Semail Ophiolite (Oman) and averages 1690 ± 714 mm/year (1985–2024) (Figure 3).

4.2 | Physicochemical Characteristics

4.2.1 | Cold Continental Sites

The Tablelands massif is notable for its extended period of serpentinization, which began with tectonic uplift and emplacement during the Middle Ordovician, approximately 500 million years ago (Cook et al. 2021). The massif consists of partially to completely serpentinised ultramafic peridotites (harzburgite with minor lherzolites), mafic lithologies, and sedimentary rocks (Szponar et al. 2013). The hyperalkaline fluids within the Tablelands massif display the highest reported dissolved $GeoH_2$ concentration across all locations, with a maximum of 3.24 mmol/L, substantially higher than the maximum dissolved CH_4 concentration of 0.06 mmol/L (Winter House Canyon seepage; Cumming et al. 2019). The average pH is also the highest among the sites (12.26 ± 0.33) (Szponar et al. 2013; Morrill et al. 2014; Cumming et al. 2019; Cook et al. 2021). The geochemical composition is characteristic of Type II hyperalkaline fluids, marked by notably elevated concentrations of K^+ (20.20 mmol/L), Na^+ (8.79–39.00 mmol/L), and Cl^- (9.06 ± 4.10 mmol/L) relative to the other sites (Szponar et al. 2013; Cook et al. 2021).

The Soldatskaya Mt. in the Kamchatsky Mys comprises 70 km^2 of peridotite sheets (harzburgites, lherzolites, and dunites)

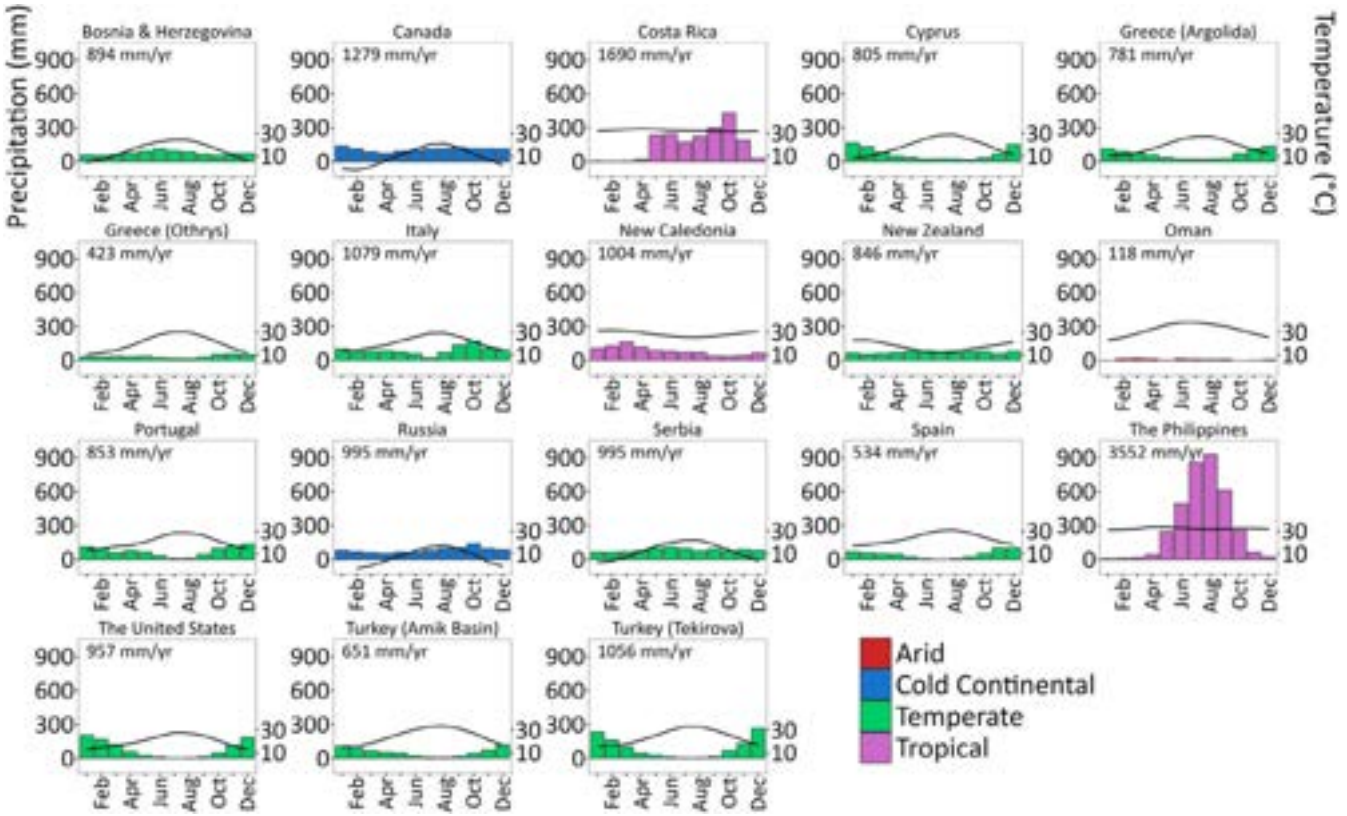

FIGURE 3 | Climographs showing monthly and mean annual precipitation (mm; bar graph) and air temperature (°C; line graph) seasonality in arid (red), cold continental (blue), temperate (green), and tropical (purple) serpentinization-influenced sites.

ranging from completely serpentinised to almost fresh peridotite (< 0.5% serpentine) (Batanova et al. 2014; Taran et al. 2024). Numerous hyperalkaline springs have been identified along the Belaya River, and their geochemical signatures are typical of Type II hyperalkaline fluids. This site exhibits the coldest spring temperatures recorded (5.79°C ± 1.13°C), with dissolved $GeoH_2$ also present at concentrations of 0.25 ± 0.35 mmol/L (Taran et al. 2024).

4.2.2 | Temperate Sites

The Dinaric-Hellenic and Vardar Zones ophiolites, which extend for 1000 km and range from 100 to 150 km in width, constitute the largest ophiolite belt in Europe (Spahić et al. 2023). Hyperalkaline seepages influenced by serpentinization have been identified in Bosnia and Herzegovina (Dinaride ophiolite belt; Etiope et al. 2017), western Serbia (Inner Dinaric and Vadar Zone ophiolite belts; Spahić et al. 2023), and Greece (Othrys and Argolida ophiolites; Etiope, Tsikouras, et al. 2013; Etiope, Vance, et al. 2013; D'Alessandro et al. 2018; Li Vigni et al. 2021). The ultramafic rocks of the Othrys ophiolite, mainly harzburgites, exhibit variable degrees of alteration, ranging from 20% to 80% (Etiope, Tsikouras, et al. 2013; Etiope, Vance, et al. 2013). The hyperalkaline springs and seepages located in the Dinaric-Hellenic and Vardar Zones ophiolites display typical Type II fluid chemistry. Notably, the Dinaride fluids have high levels of dissolved CH_4 (maximum 2.71 mmol/L) and moderate concentrations of dissolved $GeoH_2$ (maximum 0.35 mmol/L) (Etiope et al. 2017). Located in southern Spain, the Ronda peridotite massifs are among the world's largest outcrops of subcontinental mantle (450 km^2) (Ojeda et al. 2023). The Ronda massifs, mainly composed of spinel and plagioclase peridotites, typically have a degree of serpentinization < 30% of the total rock volume (Villasante-Marcos et al. 2003; Giampouras et al. 2019). Dissolved gas measurements from the associated hyperalkaline fluids show maximum concentrations of 0.60 mmol/L $GeoH_2$ and 0.20 mmol/L CH_4 (Etiope et al. 2016; Ojeda et al. 2023). The Dun Mountain Ophiolite Belt is a geologic feature of the South Island of New Zealand, containing chromite-bearing harzburgites with varying degrees of alteration (Pawson 2014).

The Troodos Massif, located in Cyprus, can be divided into two regions: the first, the Olympus domain, consists of partially serpentinised (~50%–70%) harzburgites with minor dunites, and the second is the Artemis domain, consisting of completely serpentinised peridotite (Evans et al. 2021). The salinity of Cyprus's hyperalkaline groundwater, particularly Na^+ at 16.75 mmol/L and Cl^- at 11.85 mmol/L, is significantly higher than that of other temperate continental sites (Neal and Shand 2002). This is hypothesised to be due to mixing with a saline end member and the dissolution of evaporative minerals such as gypsum, anhydrite, and halite (Neal and Shand 2002). The fluids in Cyprus also contain contributions from slab-derived fluids released from the subducting slab beneath the Troodos Massif, resulting in high salinity and elevated concentrations of dissolved elements such as Na, K, Li, B, Ba, Rb, Cs, Cl, and SO_4 (Evans et al. 2024). The Cabeço de Vide mineral waters emerge at the contact between the mafic/ultramafic pluton, the Alter-do-Chão massif, and carbonate metasediments of Elvas, situated in the

Ossa Morena Zone of the Iberian Hercynian belt in Central Portugal (Marques et al. 2008; Etiope, Tsikouras, et al. 2013; Etiope, Vance, et al. 2013). The Voltri Massif, a part of the Penninic ophiolites, is the largest ophiolite massif in the Alps-Appenine system, located in Northern Italy, where the peridotites are highly altered (Boulart et al. 2013).

The coastal border region of California, specifically the Coast Range, contains numerous ophiolite blocks (e.g., Barnes et al. 1967; Blank et al. 2009; Suzuki et al. 2013; Crespo-Medina et al. 2014; Cook et al. 2021). In California, the high saline spring located at The Cedars is believed to be connected to a deep groundwater source, which accounts for its high concentrations of Na^+ (~15.00 mmol/L), Cl^- (~9.00 mmol/L), K^+ (30.70–159.00 mmol/L), and EC values of 3000 μS/cm (Suzuki et al. 2013; Cook et al. 2021). The Coast Range Ophiolite Microbial Observatory (CROMO) exhibits high EC values (2900–11 200 μS/cm), as well as high concentrations of dissolved CH_4 (CSWold; 2.00 mmol/L) coupled with minor dissolved $GeoH_2$ (Crespo-Medina et al. 2014). Located along the southern coast of Turkey, within the Tekirova ophiolites, is the Chimaera Ophiolite, which is notable for its terrestrial CH_4 gas seeps (Meyer-Dombard et al. 2015; Neubeck et al. 2017). This region consists of serpentinised harzburgites with a serpentinization degree of ~30%–65% (Etiope et al. 2011). Other studies have investigated serpentinization in the Amik Basin in southern Turkey, which is the southern part of the Karasu Rift, featuring an ophiolite block, the Kizildag ophiolite, located in the westernmost area of the basin (Yuce et al. 2014; D'Alessandro et al. 2018).

4.2.3 | Arid Site

The Semail Ophiolite, situated in the Sultanate of Oman, is one of the most significant and well-exposed segments of the oceanic lithosphere, covering an area of $>10\,000\,km^2$ (Searle and Cox 1999). The mantle peridotites consist mainly of olivine, orthopyroxene, and serpentine, with ~30%–70% serpentinised (Miller et al. 2016). Calcium carbonate precipitates associated with the hyperalkaline springs appear as thin surface crusts or white-orange deposits (Chavagnac et al. 2013). The hyperalkaline seepages and springs located in the Semail Ophiolite display high fluid temperatures (29.50°C ± 4.17°C) (Barnes et al. 1978; Paukert et al. 2012; Boulart et al. 2013; Miller et al. 2016; Rempfert et al. 2017; Leong et al. 2023). The dissolved aqueous geochemistry is typical of Type II fluids, with notable high Ca^{2+} (2.21 ± 1.82 mmol/L), Na + (7.74 ± 3.29 mmol/L), Cl^- (8.42 ± 5.53 mmol/L), and Fe (5.32 ± 10.53 μmol/L) (Barnes et al. 1978; Neal and Stanger 1985; Paukert et al. 2012; Boulart et al. 2013; Miller et al. 2016; Rempfert et al. 2017). The site is distinguished by its high concentrations of dissolved $GeoH_2$ (2.90 mmol/L) and CH_4 (1.44 mmol/L) (Miller et al. 2016; Rempfert et al. 2017).

4.2.4 | Tropical Sites

The Zambales Ophiolite hosts mantle peridotite (~20%–60% serpentinised), deep crustal gabbro, ocean crust pillow basalts, and marine sedimentary formations (Cardace et al. 2015; Aquino et al. 2025). Sampling campaigns conducted in 2012 and 2013 showed a varied impact of seasonal monsoons on local springs, with some remaining unaffected while others experienced significant changes. Hyperalkaline springs have been observed along the Poon Bato River and Manleluag Springs, exhibiting the highest average fluid temperatures (32.77°C ± 2.14°C) among all the serpentinization-influenced sites (Cardace et al. 2015; Wang et al. 2022). The springs have a slightly lower pH and a more muted signature of Ca^{2+} (0.46 ± 0.54 mmol/L), Na^+ (0.90 ± 0.13 mmol/L), and Cl^- (0.48 ± 0.11 mmol/L) compared to other sites (Cardace et al. 2015; Wang et al. 2022). The highest reported dissolved $GeoH_2$ and CH_4 concentrations are 0.40 mmol/L and 0.50 mmol/L, respectively (Cardace et al. 2015). Recent studies in 2023 indicate notable changes in the geochemistry of the Poon Bato Springs due to intense monsoonal precipitation, aligning with typical Type I water characteristics (pH 9.23 ± 0.23; Mg^{2+} 1.18 ± 0.07 mmol/L; Ca^{2+} 0.13 ± 0.08 mmol/L) (Vergara et al. 2023).

The Massif du Sud ophiolite nappe is a geological formation located in the South-West Pacific Ocean at the Grand Terre, the main island in New Caledonia (Corre et al. 2023). This site is unique because it features the Prony Bay spring, which discharges meteoric water into the marine environment in the southern lagoon of New Caledonia (Monnin et al. 2014). The nappe comprises ultramafic peridotites that are partially serpentinised (~20%–80%) (Corre et al. 2023; Ulrich et al. 2020). Similar to the Zambales Ophiolite in the Philippines, the hyperalkaline springs exhibit a muted serpentinization signal, with lower pH (10.84 ± 0.19) and Ca^{2+} concentrations (0.31 ± 0.06 mmol/L) (Barnes et al. 1978; Monnin et al. 2021).

Costa Rica is situated at the convergent margin of the Cocos and Caribbean plates in Central America (Gazel et al. 2006). The Santa Elena Peninsula lies along the northwestern Pacific coast of Costa Rica within the Área de Conservación Guanacaste. The Santa Elena Nappe (hereafter SEO) consists of ultramafic peridotites that are partially to 30%–100% serpentinised alongside mafic lithologies like gabbros, dolerites, and basalts (Gazel et al. 2006; Zaccarini et al. 2011; Schwarzenbach et al. 2014). Active erosional processes in the SEO watersheds have exposed much of the peridotite. Hyperalkaline springs have been identified in the Danta, Minas, and Murciélago watersheds. Compared to the other tropical sites, the SEO springs have a slightly higher pH (11.18 ± 0.28) and moderate levels of Ca^{2+} (1.00 ± 1.00 mmol/L), Na^+ (0.95 ± 0.60 mmol/L), and Cl^- (1.06 ± 1.07 mmol/L) (Sánchez-Murillo et al. 2014; Crespo-Medina et al. 2017). The hyperalkaline springs have higher DIC (0.65 ± 0.69 mmol/L) than most serpentinization-influenced sites. Ni (1.03 ± 1.77 μmol/L) and Fe (22.71 ± 32.21 μmol/L) have been widely reported in this system (Sánchez-Murillo et al. 2014). High levels of dissolved CH_4 (maximum 1.00 mmol/L) are observed in comparison to $GeoH_2$ (maximum 0.05 mmol/L) (Crespo-Medina et al. 2017).

4.3 | Global Aqueous Geochemical Comparisons of Hyperalkaline Seepages

The lack of a global database of active continental serpentinising sites and the sporadic/truncated nature of geochemical and microbial measurements (i.e., snapshots in time and space)

have resulted in limited global site comparisons (Chavagnac et al. 2013; Schrenk et al. 2013; Barnes et al. 1978; Boulart et al. 2013; Monnin et al. 2021; Cook et al. 2021; Schwander et al. 2023). The following section presents the results of statistical pairwise comparisons of global hyperalkaline seepages.

The imputed PCA results revealed distinct geochemical patterns across climatic regions, highlighting the potential influence of hydroclimatic conditions on the surface water chemistry (Figure 4). Dimension 1 (49.7%) is dominated by major ions, EC, CO_3^{2-}, OH^-, Fe, Ni, DIC, CH_4, and $GeoH_2$, reflecting strong controls on solute and redox-related chemistry, while Dimension 2 (8.7%) is primarily associated with T_w. In the Dimension 1 versus Dimension 2 biplot, tropical sites cluster toward Ni, Fe, ORP, DIC, and Mg^{2+}, reflecting more positive ORP values and elevated metal concentrations, which are potentially derived from intense rock and soil weathering. The arid site trends toward OH^-, Cl^-, Ca^{2+}, Na^+, EC, and $GeoH_2$, consistent with evaporative concentration and higher salinity in more evolved groundwaters. Cold and temperate sites show greater variability, with hyperalkaline fluids from colder environments tending toward higher pH and $GeoH_2$. Finally, the observed correlation between pH, OH^-, and dissolved $GeoH_2$ is in agreement with numerous studies and reflects the production of $GeoH_2$ and OH^- through the oxidation of iron and water reduction, resulting in hyperalkaline conditions.

Figure 5 offers a global overview of pH, EC, ORP, alkalinity, major ions, trace elements, and $GeoH_2/CH_4$ of the hyperalkaline seepages across serpentinization-influenced sites grouped by climate type (Tables S2 and S3). Significant differences in seepage water temperatures ($p < 0.0001$) aligned with climate regimes, with warmer temperatures in tropical and arid settings, and cooler conditions in temperate and cold continental sites. In general, the hyperalkaline seepage median pH (11.1) in tropical sites was significantly lower ($p < 0.001$ to 0.0001) than in arid, cold continental, and temperate sites. This can be explained by the influence of the monsoonal rainfall regime and vigorous organic matter mineralisation, which can significantly lower pH, particularly in organic-rich and biologically active environments (Wantzen et al. 2008). Median pH values in arid and temperate settings were close to 11.5, and the highest median pH was reported in cold continental sites (> 12). Tropical ORP exhibited the largest variability with significantly more oxidative conditions (−250 mV) than temperate sites ($p < 0.001$). Temperate settings showed the most reductive conditions (−390 mV), while arid (−280 mV) and cold continental (−320 mV) sites showed similar median values.

Higher median EC were reported in arid (~1850 μS/cm) and temperate (~740 μS/cm) sites, with lower EC median values in tropical (~470 μS/cm) and cold continental (~200 μS/cm)

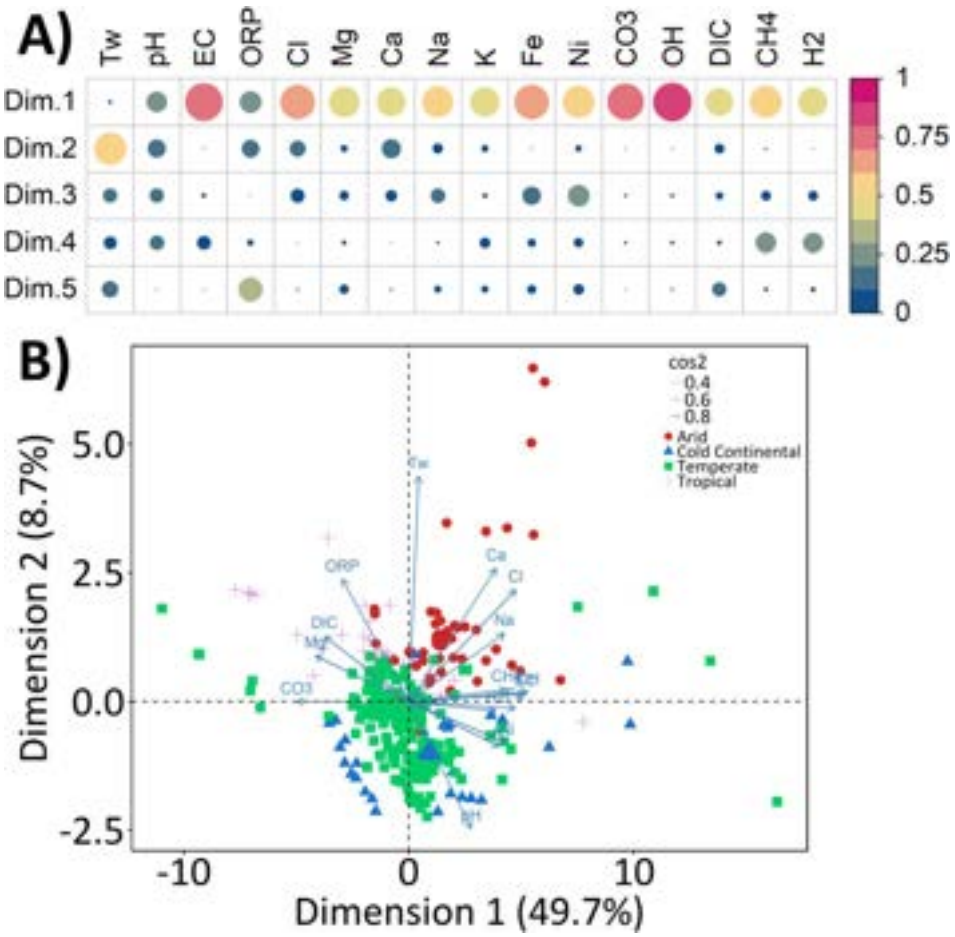

FIGURE 4 | (A) Panel showing the quality of representation of each variable on the PCA factor map, expressed as cos^2; warmer colours indicate stronger representation. (B) PCA factor map showing the first two dimensions (Dimension 1 vs. Dimension 2) for the four endmembers: arid, cold continental, temperate, and tropical, with arrows indicating variable loading and their contributions to the PCA axes.

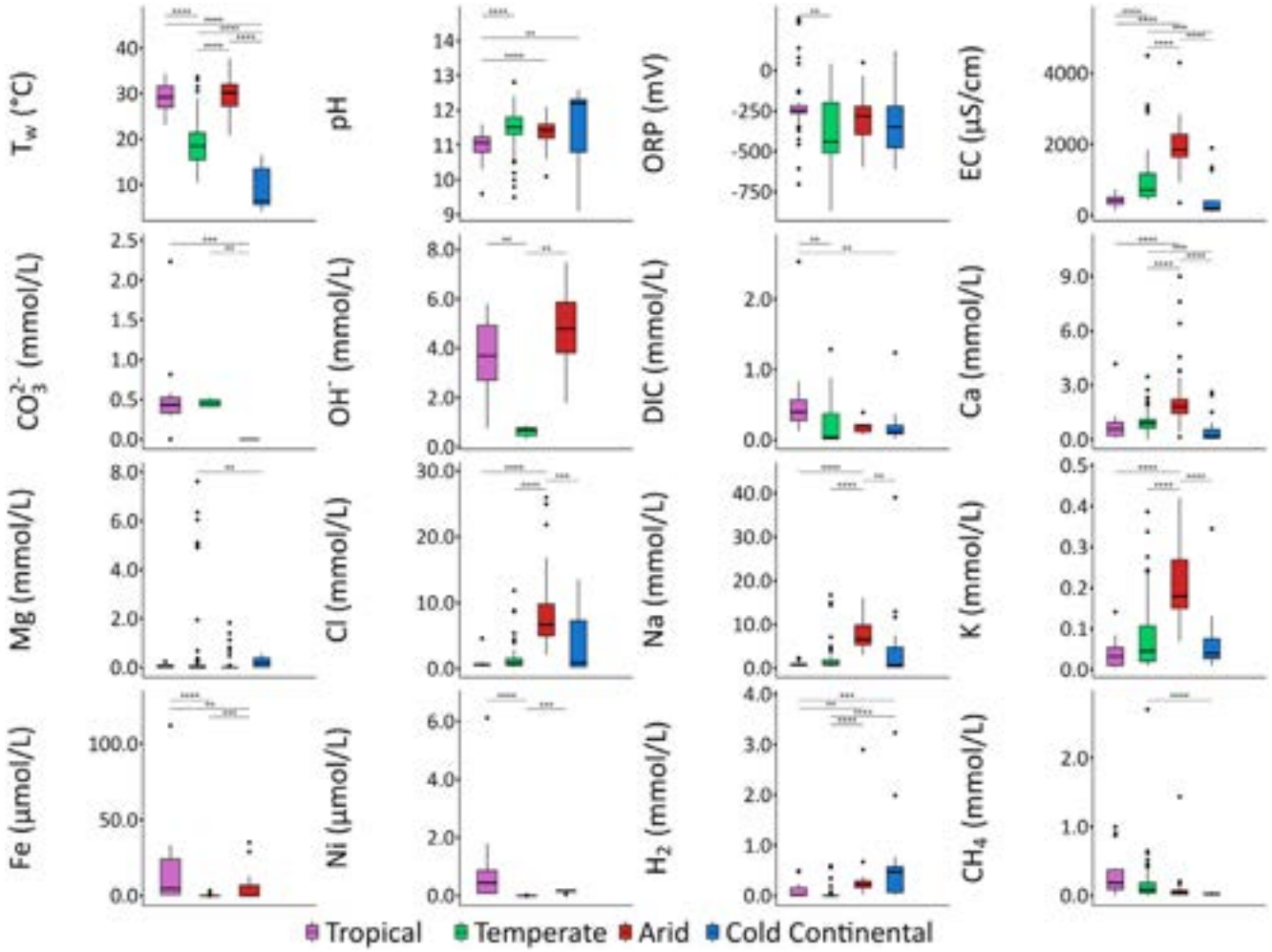

FIGURE 5 | Global comparison of pH, major ions, trace elements, and dissolved gases across serpentinization-influenced sites (hyperalkaline seepages only) (see Table 1 and Tables S2 and S3). Sites are grouped and colour-coded by climate type. Bars indicate groups that are significantly different, with asterisks denoting statistical significance: *$p < 0.05$, **$p < 0.01$, ***$p < 0.001$, and ****$p < 0.0001$. The absence of consistent measurements across sites (e.g., extended alkalinity, trace elements, gases, nutrients) limits further comparisons.

environments. The tropical and temperate sites showed significant differences ($p < 0.01$ to 0.001) in CO_3^{2-} compositions compared to arid sites. OH^- median contents were significantly higher in tropical and arid settings ($p < 0.01$) compared to temperate locations. Significantly higher median values of Na^+, K^+, Ca^{2+}, and Cl^- were reported in arid environments ($p < 0.01$ to 0.0001). Tropical sites exhibited the lowest median ion concentrations, followed by temperate and cold continental locations. The high EC and concentrations of Na^+, K^+, Ca^{2+}, and Cl^- could be linked to low meteoric input and increased evaporation, while the lower concentrations in the tropics could be the result of a dilution effect. Despite the higher median Mg^{2+} values in the cold continental group (0.2 mmol/L), similar low median contents in tropical, arid, and temperate suggest a dominant process controlling its mobilisation independently from wet/dry conditions.

In addition, dissolved Fe and Ni challenge the dilution rationale (e.g., greater water availability, lower concentrations) by showing the highest compositions in tropical sites (4.7 and 0.4 µmol/L, respectively). This may reflect the influence of lower pH, which can increase metal solubility, and/or enhanced metal mobilisation driven by intense tropical precipitation events (Bourg and Loch 1995). In the Santa Elena ophiolite in particular, unusually high Ni concentrations have been reported in soils (3000–7500 mg/kg), whereas Fe concentrations (10–16 wt%) are typical of serpentinised environments (Reeves et al. 2007). Coupled with high Fe and Ni concentrations, the tropical sites exhibit the highest median concentration of DIC in comparison to temperate, cold continental, and arid sites. Higher median concentrations of CH_4 were reported in the tropical (0.2 mmol/L) and temperate (0.1 mmol/L) sites compared to the arid and cold continental sites ($p < 0.01$ to 0.0001). In contrast, higher median $GeoH_2$ values were reported in the arid (0.2 mmol/L) and cold continental (0.5 mmol/L) sites compared to the tropical and temperate sampling locations ($p < 0.01$ to 0.0001).

4.4 | Variations in $GeoH_2$ and CH_4 in Serpentinise Environments

In serpentinising environments, significant variations in dissolved $GeoH_2$ and CH_4 concentrations have been identified.

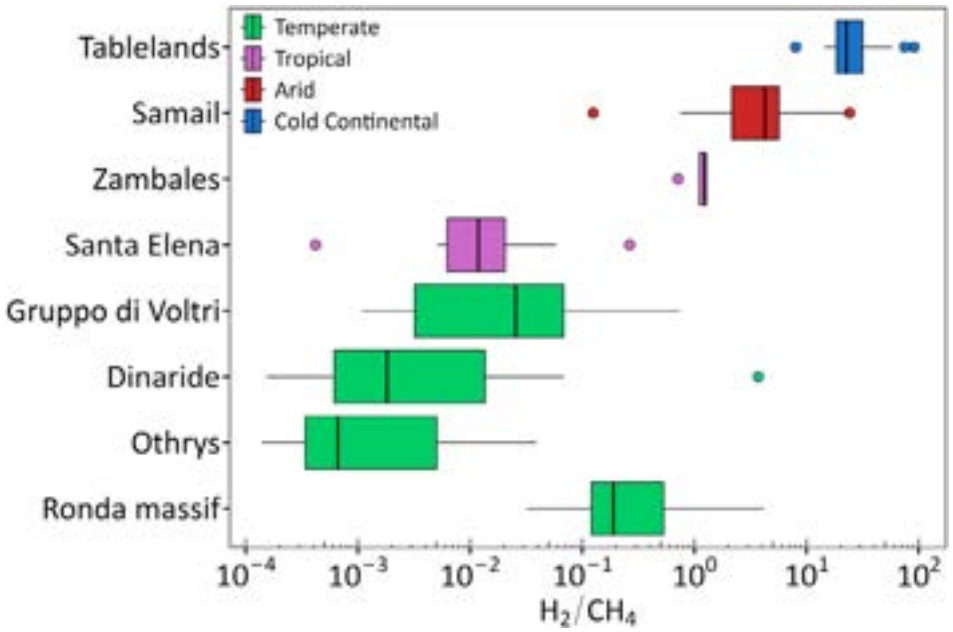

FIGURE 6 | Dissolved H_2/CH_4 ratio [dimensionless; log-scaled] in serpentinising fluids (colour-coded by the Köppen-Geiger climate classification): tropical (Cardace et al. 2015; Crespo-Medina et al. 2017; Unpublished data), Cold Continental (Szponar et al. 2013; Morrill et al. 2014; Cumming et al. 2019), arid (Boulart et al. 2013; Miller et al. 2016; Rempfert et al. 2017), and Temperate (Boulart et al. 2013; Etiope, Tsikouras, et al. 2013; Etiope, Vance, et al. 2013; Etiope et al. 2016, 2017; Ojeda et al. 2023; Li Vigni et al. 2021).

Although some sites have reported CH_4- and H_2-dominated springs (e.g., Cardace et al. 2015; Etiope et al. 2016, 2017; Miller et al. 2016), two main groups have been identified: $GeoH_2$ and CH_4-dominant (Figure 6). Temperate and tropical sites are CH_4-dominant, while the drier, arid, and cold climates of Oman and Canada are $GeoH_2$-dominant. These patterns may reflect differences in serpentinization dynamics across precipitation regimes. In wetter environments, greater subsurface fluid availability and DIC could facilitate more extensive water-rock interaction and promote CH_4 generation through abiotic and biotic processes, respectively. In particular, the Santa Elena Ophiolite in Costa Rica exhibits high CH_4 concentrations in hyperalkaline surface manifestations, associated with the highest recorded DIC levels, potentially providing a carbon source for abiotic and/or biotic CH_4 production. Conversely, in colder or more arid settings, limitations on groundwater recharge and temperature may inhibit CH_4 production, while favouring scenarios in which $GeoH_2$ persists and accumulates. One mechanism that could explain this is the dependence of H_2 diffusivity and absorption on water temperature. Lower temperatures reduce H_2 diffusivity while increasing the absorption coefficient, thereby limiting H_2 loss and promoting the persistence and accumulation of dissolved H_2 in colder systems (Wiebe and Gaddy 1934; Alafnan 2024). Nonetheless, geological and microbial factors are likely to modulate these outcomes. Under wetter conditions, H_2 oxidation may emerge as an important microbial metabolic pathway, with microbes drawing down $GeoH_2$. Rock composition and the presence of secondary minerals, particularly the availability of Fe^{2+}, further influences H_2 generation. To address interactive controls, a more comprehensive sampling strategy is recommended to evaluate the integration of geological, hydrological, and microbial controls on $GeoH_2$ and CH_4 production and consumption.

5 | Discussion

5.1 | Physicochemical, Mineralogical, and Microbiological Controls on $GeoH_2$ and CH_4 Production

Multiple studies have alluded that the generation of $GeoH_2$, and thus indirectly the availability of abiotic/biotic CH_4, is modulated by temperature, pressure, water-rock ratios, catalytically active minerals, the composition of the parent material, and chemosynthetic microorganisms (Sleep et al. 2004; McCollom and Bach 2009; Evans et al. 2013; Mayhew et al. 2013; Klein et al. 2013; Tiago and Veríssimo 2013; Schrenk et al. 2013; Foustoukos et al. 2015; Crespo-Medina et al. 2017; Lamadrid et al. 2017; Neubeck et al. 2017; Barbier et al. 2020; Leong et al. 2023). Thermodynamic modelling and experimental studies demonstrate that $GeoH_2$ production is most favourable at temperatures between 200°C and 315°C, is kinetically limited and requires long timescales at lower temperatures, and halts above 350°C due to olivine stability (McCollom and Bach 2009).

The composition of the ultramafic rocks also plays a role in $GeoH_2$ production. Thermodynamic modelling by Klein et al. (2013) demonstrates that fayalite-rich olivine (high in Fe^{2+}) remains stable at lower temperatures ($\leq$180°C) compared to forsterite-rich olivine (low in Fe^{2+}), resulting in higher predicted $GeoH_2$ availability from serpentinization under low temperature conditions. Furthermore, accessory metal-bearing minerals and alloys (e.g., Fe, Ni, Cr Co) play a catalytic role in facilitating abiotic CH_4 formation via Fisher-Tropsch-type reactions (e.g., the Sabatier reaction), particularly at elevated temperatures ($>$150°C–200°C) (Sleep et al. 2004; Evans et al. 2013; Foustoukos et al. 2015; Preiner et al. 2018; Etiope and Whiticar 2019). In some low-temperature environments ($<$100°C), chromitites

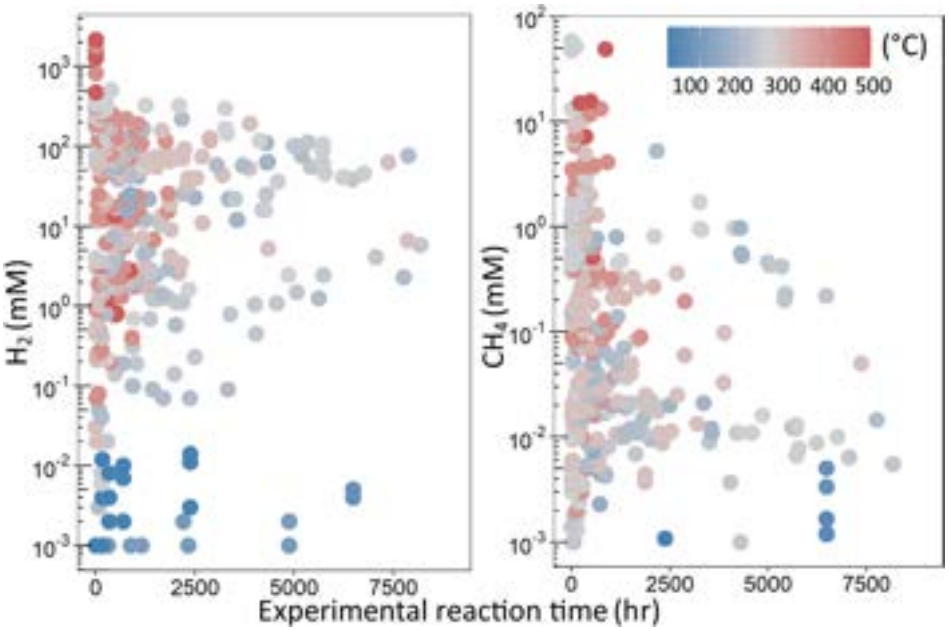

FIGURE 7 | H_2 and CH_4 laboratory-based dissolved concentrations versus experimental reaction time (hours) (modified after Barbier et al. 2020). Reaction temperature is colour-coded in °C.

may provide metal catalysts (e.g., Ru), facilitating abiotic CH_4 production via the Sabatier reaction (Etiope and Ionescu 2015; Etiope and Whiticar 2019).

Multiple laboratory-based serpentinization tests to mimic natural hydrogeological conditions and elucidate key drivers leading to abiotic $GeoH_2$ and CH_4 production (Figure 7, modified after Barbier et al. 2020). $GeoH_2$ and CH_4 production in these controlled experiments is thermodynamically constrained by temperature (testing range = 25°C–500°C) and pressure (testing range = 0.1–350 MPa). Nevertheless, the experimental reaction times (up to ca. 11 months) do not represent water transit time in natural hydrogeological settings (Benettin et al. 2022). In addition, experimental parameters ($n > 100$) varying from one experiment to another have precluded a confident assessment of the large variance observed in both $GeoH_2$ and CH_4 concentrations, spanning six orders of magnitude (10^{-3}–10^{3} mmol/L). Despite the lack of an external heat source and low temperatures (< 50°C–100°C), relatively high levels of $GeoH_2$ and CH_4 have been reported in hyperalkaline seepages at various global sites, with a mean value of 0.2 mmol/L for both species. Interestingly, the highest recorded CH_4 in a hyperalkaline surface manifestation is at the SEO in Costa Rica (1.0 mmol/L), underscoring the need to understand the overall impact of monsoonal stimulation on $GeoH_2$ and CH_4 production.

5.2 | The Role of Fluid Chemistry and Water Availability

Fluid chemistry, water-rock ratios, and water availability strongly regulate serpentinization rates and $GeoH_2$ production. Numerical modelling by McCollom and Bach (2009) shows that higher water-rock ratios increase the total amount of $GeoH_2$ produced per kg of rock but yield lower dissolved $GeoH_2$ concentration due to a dilution effect, and less water is incorporated into hydrated minerals, while at lower water-rock ratios, less $GeoH_2$ is generated, but it becomes more concentrated due to less dilution and greater water incorporated into minerals.

In addition to the water-rock ratio, fluid salinity and water availability exert strong controls on reaction rates, with lower salinity and higher dilution conditions enhancing reactions. Experimental work by Lamadrid et al. (2017) demonstrated that increasing fluid salinity suppresses olivine serpentinization by lowering H_2O activity, resulting in slower reaction rates under otherwise identical temperature conditions (280°C). Complementary continuous-flow experiments by Ross et al. (2025) further show that sustained fluid supply promotes olivine dissolution and $GeoH_2$ generation while facilitating serpentine precipitation, keeping flow pathways open, and allowing sustained $GeoH_2$ generation throughout the experiment. These findings highlight the role of water availability and salinity in sustaining $GeoH_2$ production. Consequently, natural systems characterised by persistent recharge and low salinity fluids may sustain $GeoH_2$ production over longer periods than systems dominated by low recharge and saline fluids.

Despite extensive literature regarding $GeoH_2$ and CH_4 production in serpentinising environments, the role of water transit time, specifically the water age from recharge to the seepage outlet, remains poorly constrained and underexplored (Hrachowitz et al. 2016). Additionally, there is limited information on site-specific ophiolitic aquifers. In a pioneering effort, Dewandel et al. (2005) aimed to develop a conceptual hydrogeological model of ophiolitic hard rock aquifers in Oman, but subsurface flow paths, recharge, extension of the system, age distribution, water transit time, and the geologic composition of these aquifer systems are still poorly understood. Similarly, seasonally dependent processes, such as wetting and drying cycles in non-perennial streams and springs in serpentinising environments, have received limited attention with respect to their role in $GeoH_2$/CH_4 production and microbial activity. As a result, our understanding of how hydrological variability modulates redox

conditions, solute mobility, mineral alteration, and microbial metabolism in active ultramafic systems remains incomplete.

Adding further complexity is the role of stream and groundwater hydrology in serpentinising systems, particularly where seasonal hydrological transitions control surface-subsurface connectivity, groundwater infiltration, and subsurface flow paths, thereby regulating dissolved gas concentrations, carbon availability (e.g., DIC), fluid chemistry, and redox conditions. Rewetting events can mobilise gases and solutes accumulated during dry periods, supply new carbon sources, alter redox conditions, and trigger microbial processes, while prolonged drying can reduce biotic activity (Datry et al. 2023; Price et al. 2024). Furthermore, water age, precipitation seasonality, and consequently the transport and mixing of other carbon solutes are key variables to fully decompose the enigmatic $GeoH_2/CH_4$ concentration and isotopic alterations. While these mechanisms are relatively well-studied in perennial streams, non-perennial streams, particularly in geologically distinct settings such as ophiolites, remain poorly understood. For example, in systems like the Santa Elena Ophiolite in Costa Rica, where the hydrological year is defined by wet and dry cycles, the unique geochemistry of hyperalkaline and surface fluids, as well as the intermittent nature of springs and streams, may strongly modulate these hydrological and biogeochemical cycles, influencing microbial activity, solute transport, and ecosystem responses.

5.3 | Challenges in Distinguishing Abiotic Versus Biotic CH_4

Challenges arise when determining the abiotic/biotic origin of the CH_4 produced across serpentinization-influenced sites on land. CH_4 can be produced through various processes, including thermogenic degradation of organic matter in sedimentary rocks ($\delta^{13}C$ −50 to −20‰; $\delta^{2}H$ −275 to −100‰; Whiticar 1999), microbial methanogenesis by methanogens ($\delta^{13}C$ −110 to −50‰; $\delta^{2}H$ −400 to −150‰; Whiticar 1999), and abiotic production through FTT synthesis ($\delta^{13}C > -40$‰; $\delta^{2}H$ −400 to −100‰; Etiope and Oze 2022; Ojeda et al. 2023). The presence of heavier hydrocarbons (e.g., propane, ethane), the absence of ^{14}C in CH_4, and the presence of metal catalysts are also indicators of abiotic CH_4 (Etiope and Oze 2022; Ojeda et al. 2023). Abiotic and biotic CH_4 have similar and overlapping carbon and hydrogen isotopic compositions and often, in natural systems, contain CH_4 from multiple sources. Furthermore, temperature, pressure, and geochemical conditions can affect CH_4 formation and isotopic fractionation, and post-formation processes can alter the original isotopic composition of CH_4 (Whiticar 1999; Proskurowski et al. 2008; McCollom and Seewald 2013; Etiope and Sherwood Lollar 2013; Etiope and Whiticar 2019; Etiope and Oze 2022; Ojeda et al. 2023).

The serpentinization process produces conditions that may support biogenic CH_4 production by chemolithoautotrophic microorganisms, but the relative contributions of abiogenic versus biogenic methanogenesis remain unclear and are still debated (Blank et al. 2009; McCollom and Seewald 2013; Crespo-Medina et al. 2017; Etiope and Oze 2022; Schwander et al. 2023). A strong microbial contribution could be attributed to low ^{13}C-CH_4 values ($\delta^{13}C < -50$‰) in some hyperalkaline springs (Bosnia, Spain, California, Costa Rica). Recent research suggests that microbial CH_4 production can also lead to enriched ^{13}C-CH_4 values in H_2-rich, CO_2-limited hyperalkaline environments, where methanogens convert most of the limited CO_2 into CH_4, decreasing carbon isotope fractionation and resulting in relatively enriched ^{13}C-CH_4 values (Nothaft et al. 2021; Etiope and Oze 2022; Howells et al. 2025).

Figure 8 illustrates the complexity of identifying CH_4 sources in serpentinised environments, showing $\delta^{13}C$-CH_4 (‰-VPDB) compositions plotted against pH, with symbol size proportional to CH_4 concentration (mmol/L). Commonly, reported CH_4 concentrations reached up to ~0.50 mmol/L, except for relatively high values in Costa Rica (Murciélago seepages, SEO) (1.00 mmol/L) (Crespo-Medina et al. 2017) and two deep systems in Bosnia and Oman (boreholes and wells, ranging from 18 m to 670 m depth) (1.14 to 2.70 mmol/L) (Miller et al. 2016; Etiope et al. 2017). Isotopically, $\delta^{13}C$ values ranged from high in Oman (Semail) and Costa Rica (Murciélago; surface water and spring seepages) to low compositions in Spain (Ronda), the Coast Range (California, USA), and Bosnia. Other sites denote a large potential mixing between abiotic and biotic sources (Whiticar 1999; Etiope and Sherwood Lollar 2013). Although the significant variability in $\delta^{13}C$-CH_4 may reflect the processes described above, most existing studies rely on single sampling campaigns focused on mineralogical and microbial characterisation. This limits the ability to assess how $\delta^{13}C$-CH_4 varies over time, particularly in response to seasonal transitions between wet and dry periods. Therefore, a holistic approach is necessary, combining multiple data sources such as gas and water chemistry, mineralogy, seasonal hydrology, and microbiology, to better understand the source and formation of CH_4 and $GeoH_2$ (Ojeda et al. 2023).

6 | Conclusions and Future Research

In summary, there are many enigmatic or unclear constraints on continental serpentinization. In particular, hydrological influences remain poorly understood. Although water is a primary reactant driving serpentinization reactions, it is often treated as a time-invariant factor. However, several hydrogeological features, including watershed unsaturated versus saturated conditions, subsurface storage, precipitation variability, and groundwater flow in confined/unconfined or perched aquifers, vary in time and space across watersheds. Water availability differences may lead to changes in water-rock ratios, oxidation and reduction conditions, high or low salinity, dilution effects, water activity, and microbial activity. Additionally, the temporal and spatial evolution of serpentinization is unclear, especially regarding the occurrence of patchy hyperalkaline seepages on land throughout the hydrological year. Subsurface features such as faults, fractures, and peridotite/dikes/conglomerates contact zones may be relevant in facilitating preferential groundwater flowpaths across fresh unreacted rocks.

Furthermore, a significant portion of the research on low temperature serpentinization systems has been conducted as a singular snapshot, lacking the incorporation of seasonal or intra-seasonal sampling. Serpentinization systems are inherently dynamic environments influenced by both geochemical

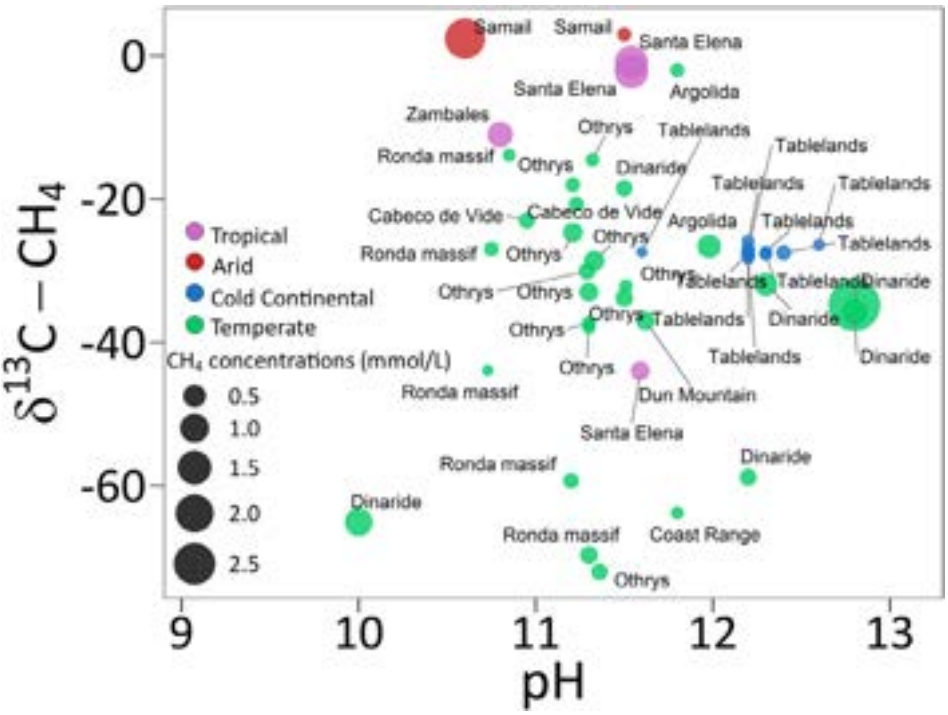

FIGURE 8 | pH versus $\delta^{13}C$-CH_4 in serpentinising fluids, with symbol size proportional to dissolved CH_4 concentration (mmol/L) and colour-coded by Köppen-Geiger climate classification: Argolida (D'Alessandro et al. 2018), Cabeço de Vide (Marques et al. 2018), Coast Range (Cook et al. 2021), Dinaride (Etiope et al. 2017), Dun Mountain (Pawson 2014), Zambales (Crespo-Medina et al. 2017), Santa Elena (Crespo-Medina et al. 2017), Othrys (Etiope, Tsikouras, et al. 2013; Etiope, Vance, et al. 2013; Li Vigni et al. 2021), Ronda massif (Etiope et al. 2016), Semail (Miller et al. 2016), and Tablelands (Szponar et al. 2013; Cumming et al. 2019).

processes and external environmental drivers (e.g., precipitation and/or snowfall events, seasonal recharge, local and regional groundwater flows), which can induce rapid and significant changes in the flow regime, solute transport, and microbial activity. These changes are often episodic and short-lived, making them difficult to capture with infrequent or one-time sampling efforts. During wet periods, increased precipitation and infiltration can alter pH, redox conditions, water chemistry, and fluid–rock interaction pathways by introducing oxic waters or by flushing accumulated solutes. However, dry periods may increase surface evaporation, reducing effective recharge and thereby decreasing water availability to the subsurface system. These seasonal shifts could indirectly influence CH_4 and $GeoH_2$ production rates and alter associated microbial communities. Therefore, if the sampling conducted is a single snapshot of the system, it may provide a misleading representation of gas production dynamics and microbial activity. In order to fully understand serpentinising systems, sampling requires capturing data (e.g., hydrological, geochemical, petrological, and geobiological) at multiple points across the hydrological year (e.g., baseflow period, peak wet season, transitional periods). Without such data, gas and trace elements flux determinations as well as model conceptualisations of active serpentinization remain incomplete.

In the literature, knowledge gaps prevail concerning the impact of water transit time and the complex seasonal processes that influence $GeoH_2$ and carbon cycling in serpentinised environments at the watershed scale. Chavagnac et al. (2013) investigated the fluid chemistry of hyperalkaline spring waters in both Oman and Liguria and found that the chemistry has remained stable over time, despite changes in groundwater levels, concluding that hyperalkaline spring chemistry is strongly controlled by subsurface processes and insensitive to short-term hydrological variability. However, tropical systems may behave differently as pronounced wet-dry cycles could lead to greater fluctuations in water chemistry and dissolved gas concentrations. For example, Meyer-Dombard et al. (2019) show how seasonal precipitation affects the subsurface geochemical signature of springs in the Zambales and Palawan ophiolites by analysing carbon and nitrogen isotopes in fluids and solid materials across springs with different flow rates during the wet and dry seasons. The study found that seasonal rainfall shifts $\delta^{13}C$ values, with the high-flow systems being more influenced by surface inputs and low-flow systems retaining stronger subsurface carbon signatures. Dry-season conditions and low-flow systems amplify subsurface signals, making them ideal sites for investigating subsurface processes.

Additionally, there are limited studies in the literature applying groundwater dating techniques to constrain the apparent age of hyperalkaline systems. Marques et al. (2008) applied isotopic dating techniques (^3H, ^{13}C, ^{14}C) to the Cabeço de Vide waters in Portugal. The absence of ^3H indicated that the waters were older than 60 years, while ^{13}C and ^{14}C yielded an apparent age of 2790 ± 40 a BP. Similarly, Cipolli et al. (2004) applied ^3H dating to the Gruppo di Voltri waters in Italy. Their findings suggested that these high-pH waters have long residence times (100–10 000 years). However, in tropical settings, groundwater systems may be more sensitive to intense monsoonal precipitation, resulting in comparatively younger apparent groundwater ages.

To conclude, our statistical results reveal significant differences in hyperalkaline fluid aqueous chemistry and dissolved

gases across the global sites. However, the limited seasonal characterisation of geochemical, mineralogical, and microbial aspects in these systems hinders a full understanding of the key controls of $GeoH_2$ and CH_4 production and consumption rates. Future research should prioritise integrated, seasonality-based studies combining hydrology, geochemistry, mineralogy, and microbiology, as these approaches are critical for elucidating the main drivers of $GeoH_2$ production in serpentinising environments.

Acknowledgements

This research was supported by the University of Texas System STARs Program (no. AR911486 to RSM), The University of Texas-Arlington (UTA) Office of the Provost (no. 314075 to R.S.M.), the UTA's College of Science Research Enhancement and Innovation Seed grant (no. 31478 to R.S.M.), the UTA's Graduate School Maverick Merit Fellowship and Krishnan Rajeshwar and Rohini Krishnan Graduate Fellowship to A.M. Sampling within the Santa Elena Ophiolite was possible via a research permit from the Guanacaste Conservation Area, the Costa Rican National Parks System, and the National Council of Biodiversity (R-042-2025-OT-CONAGEBIO to RSM). The authors recognise the valuable assistance from the Guanacaste Conservation Area personnel in coordinating field expeditions logistics. E.G. is a member of the scientific board for Vema Hydrogen, and a founder and board member of Hydronova Energy.

Funding

This work was supported by University of Texas System STARs Program (AR911486), The University of Texas-Arlington (UTA) Office of the Provost (314075) and UTA's College of Science Research Enhancement and Innovation Seed (31478), UTA's Graduate School Maverick Merit Fellowship, and Krishnan Rajeshwar and Rohini Krishnan Graduate Fellowship.

Data Availability Statement

The data that support the findings of this study are openly available in HydroShare at https://www.hydroshare.org/resource/9ad700ebb18947e3a49662d78dfaa21b/.

References

Abrajano, T. A., N. C. Sturchio, J. K. Bohlke, G. L. Lyon, R. J. Poreda, and C. M. Stevens. 1988. "Methane-Hydrogen Gas Seeps, Zambales Ophiolite, Philippines: Deep or Shallow Origin?" *Chemical Geology* 71: 211–222. https://doi.org/10.1016/0009-2541(88)90116-7.

Abrajano, T. A., N. C. Sturchio, B. M. Kennedy, G. L. Lyon, K. Muehlenbachs, and J. K. Bohlke. 1990. "Geochemistry of Reduced Gas Related to Serpentinization of the Zambales Ophiolite, Philippines." *Applied Geochemistry* 5, no. 5–6: 625–630. https://doi.org/10.1016/0883-2927(90)90060-I.

Alabaster, T., J. A. Pearce, and J. Malpas. 1982. "The Volcanic Stratigraphy and Petrogenesis of the Oman Ophiolite Complex." *Contributions to Mineralogy and Petrology* 81, no. 3: 168–183.

Alafnan, S. 2024. "Assessing Leakage Risks of Hydrogen Through Aquifers and Caprocks." *Energy & Fuels* 38, no. 20: 19739–19747. https://doi.org/10.1021/acs.energyfuels.4c03228.

American Public Health Association, American Water Works Association, and Water Environment Federation. 2024. *Standard Methods for the Examination of Water and Wastewater: Methods 4110 and 5310*, edited by W. C. Lipps, T. E. Baxter, and E. Braun-Howland. APHA Press. https://doi.org/10.2105/SMWW.2882.002.

Aquino, K. A., A. d. C. Perez, C. M. M. Juego, Y. G. M. Tagle, J. A. M. Leong, and E. A. Codillo. 2025. "High Hydrogen Outgassing From an Ophiolite-Hosted Seep in Zambales, Philippines." *International Journal of Hydrogen Energy* 105: 360–366. https://doi.org/10.1016/j.ijhydene.2025.01.251.

Arsenović, P., I. Tošić, and M. Unkašević. 2015. "Trends in Combined Climate Indices in Serbia From 1961 to 2010." *Meteorology and Atmospheric Physics* 127, no. 4: 489–498. https://doi.org/10.1007/s00703-015-0380-6.

Barbier, S., F. Huang, M. Andreani, et al. 2020. "A Review of H_2, CH_4, and Hydrocarbon Formation in Experimental Serpentinization Using Network Analysis." *Frontiers in Earth Science* 8: 209. https://doi.org/10.3389/feart.2020.00209.

Barnes, I., V. C. Lamarche, and G. Himmelberg. 1967. "Geochemical Evidence of Present-Day Serpentinization." *Science* 156, no. 3776: 830–832. https://doi.org/10.1126/science.156.3776.830.

Barnes, I., J. R. Oneil, and J. J. Trescases. 1978. "Present Day Serpentinization in New Caledonia, Oman and Yugoslavia." *Geochimica et Cosmochimica Acta* 42: 144–145. https://doi.org/10.1016/0016-7037(78)90225-9.

Batanova, V. G., Z. E. Lyaskovskaya, G. N. Savelieva, and A. V. Sobolev. 2014. "Peridotites From the Kamchatsky Mys: Evidence of Oceanic Mantle Melting Near a Hotspot." *Russian Geology and Geophysics* 55: 1395–1403. https://doi.org/10.1016/j.rgg.2014.11.004.

Benettin, P., N. B. Rodriguez, M. Sprenger, et al. 2022. "Transit Time Estimation in Catchments: Recent Developments and Future Directions." *Water Resources Research* 58, no. 11. https://doi.org/10.1029/2022WR033096.

Blank, J. G., S. J. Green, D. Blake, et al. 2009. "An Alkaline Spring System Within the Del Puerto Ophiolite (California, USA): A Mars Analog Site." *Planetary and Space Science* 57, no. 5–6: 533–540. https://doi.org/10.1016/j.pss.2008.11.018.

Boschetti, T., and L. Toscani. 2008. "Springs and Streams of the Taro-Ceno Valleys (Northern Apennine, Italy): Reaction Path Modeling of Waters Interacting With Serpentinized Ultramafic Rocks." *Chemical Geology* 257, no. 1–2: 76–91. https://doi.org/10.1016/j.chemgeo.2008.08.017.

Boschetti, T., L. Toscani, P. Iacumin, and E. Selmo. 2017. "Oxygen, Hydrogen, Boron and Lithium Isotope Data of a Natural Spring Water With an Extreme Composition: A Fluid From the Dehydrating Slab?" *Aquatic Geochemistry* 23, no. 5–6: 299–313. https://doi.org/10.1007/s10498-017-9323-9.

Boulart, C., V. Chavagnac, C. Monnin, A. Delacour, G. Ceuleneer, and G. Hoareau. 2013. "Differences in Gas Venting From Ultramafic-Hosted Warm Springs: The Example of Oman and Voltri Ophiolites." *Ofioliti* 38, no. 2: 143–156. https://doi.org/10.4454/ofioliti.v38i2.423.

Bourg, A. C. M., and J. P. G. Loch. 1995. "Mobilization of Heavy Metals as Affected by pH and Redox Conditions." In *Biogeodynamics of Pollutants in Soils and Sediments. Environmental Science*, edited by W. Salomons and W. M. Stigliani. Springer. https://doi.org/10.1007/978-3-642-79418-6_4.

Brazelton, W. J., B. Nelson, and M. O. Schrenk. 2012. "Metagenomic Evidence for H_2 Oxidation and H_2 Production by Serpentinite-Hosted Subsurface Microbial Communities." *Frontiers in Microbiology* 2: 268. https://doi.org/10.3389/fmicb.2011.00268.

Cardace, D., D. R. Meyer-Dombard, K. M. Woycheese, and C. A. Arcilla. 2015. "Feasible Metabolisms in High pH Springs of the Philippines." *Frontiers in Microbiology* 6: 10. https://doi.org/10.3389/fmicb.2015.00010.

Chavagnac, V., C. Monnin, G. Ceuleneer, C. Boulart, and G. Hoareau. 2013. "Characterization of Hyperalkaline Fluids Produced by Low Temperature Serpentinization of Mantle Peridotites in the Oman and Ligurian Ophiolites." *Geochemistry, Geophysics, Geosystems* 14, no. 7: 2496–2522. https://doi.org/10.1002/ggge.20147.

Chibati, N., Y. Géraud, and K. S. Essa. 2022. "Petrophysical Characterization and Thermal Conductivity Prediction of Serpentinized Peridotites." *Geophysical Journal International* 231, no. 3: 1786–1805. https://doi.org/10.1093/gji/ggac288.

Christiansen, R., G. Gabriel, and M. Sobh. 2024. "Integrated Methodologies for Estimating Natural Hydrogen Generation in Serpentinization Environments." *AGU Fall Meeting Abstracts* 2024: 1196.

Cipolli, F., B. Gambardella, L. Marini, G. Ottonello, and M. V. Zuccolini. 2004. "Geochemistry of High-pH Waters From Serpentinites of the Gruppo di Voltri (Genova, Italy) and Reaction Path Modeling of CO_2 Sequestration in Serpentinite Aquifers." *Applied Geochemistry* 19, no. 5: 787–802. https://doi.org/10.1016/j.apgeochem.2003.10.007.

Coleman, R. G. 1971. "Petrologic and Geophysical Nature of Serpentinites." *Geological Society of America Bulletin* 82, no. 4: 897–918. https://doi.org/10.1130/00167606(1971)82[897:pagnos]2.0.co;2.

Coleman, R. G. 1977. "Ophiolites: Ancient Oceanic Lithosphere?" In *Minerals, Rocks, and Mountains*, 1st ed. Springer. https://doi.org/10.1007/978-3-642-66673-5.

Cook, M. C., J. G. Blank, A. Rietze, S. Suzuki, K. H. Nealson, and P. L. Morrill. 2021. "A Geochemical Comparison of Three Terrestrial Sites of Serpentinization: The Tablelands, the Cedars, and Aqua de Ney." *Journal of Geophysical Research – Biogeosciences* 126, no. 11: 316. https://doi.org/10.1029/2021JG006316.

Corre, M., F. Brunet, S. Schwartz, C. Gautheron, A. Agranier, and S. Lesimple. 2023. "Quaternary Low Temperature Serpentinization and Carbonation in the New Caledonia Ophiolite." *Scientific Reports* 13, no. 1: 19413. https://doi.org/10.1038/s41598-023-46691-y.

Cox, M. E., J. Launay, and J. P. Paris. 1982. "Of Low Temperature Geothermal Systems in New Caledonia."

Crespo-Medina, M., K. I. Twing, M. D. Y. Kubo, et al. 2014. "Insights Into Environmental Controls on Microbial Communities in a Continental Serpentinite Aquifer Using a Microcosm-Based Approach." *Frontiers in Microbiology* 5: 604. https://doi.org/10.3389/fmicb.2014.00604.

Crespo-Medina, M., K. I. Twing, R. Sánchez-Murillo, W. J. Brazelton, T. M. McCollom, and M. O. Schrenk. 2017. "Methane Dynamics in a Tropical Serpentinizing Environment: The Santa Elena Ophiolite, Costa Rica." *Frontiers in Microbiology* 8: 916. https://doi.org/10.3389/fmicb.2017.00916.

Cumming, E. A., A. Rietze, L. S. Morrissey, et al. 2019. "Potential Sources of Dissolved Methane at the Tablelands, Gros Morne National Park, NL, CAN: A Terrestrial Site of Serpentinization." *Chemical Geology* 514: 42–53. https://doi.org/10.1016/j.chemgeo.2019.03.019.

D'Alessandro, W., K. Daskalopoulou, S. Calabrese, and S. Bellomo. 2018. "Water Chemistry and Abiogenic Methane Content of a Hyperalkaline Spring Related to Serpentinization in the Argolida Ophiolite (Ermioni, Greece)." *Marine and Petroleum Geology* 89: 185–193. https://doi.org/10.1016/j.marpetgeo.2017.01.028.

Datry, T., A. J. Boulton, K. Fritz, et al. 2023. "Non-Perennial Segments in River Networks." *Nature Reviews Earth & Environment* 4, no. 12: 815–830. https://doi.org/10.1038/s43017-023-00495-w.

de Moor, J. M., P. H. Barry, A. Rodríguez, et al. 2025. "Origins and Fluxes of Gas Emissions From the Central Volcanic Zone of the Andes." *Journal of Volcanology and Geothermal Research* 466: 108382. https://doi.org/10.1016/j.jvolgeores.2025.108382.

Deville, E., and A. Prinzhofer. 2016. "The Origin of N2-H2-CH4-Rich Natural Gas Seepages in Ophiolitic Context: A Major and Noble Gases Study of Fluid Seepages in New Caledonia." *Chemical Geology* 440: 139–147. https://doi.org/10.1016/j.chemgeo.2016.06.011.

Dewandel, B., P. Lachassagne, F. Boudier, et al. 2005. "A Conceptual Hydrogeological Model of Ophiolite Hard-Rock Aquifers in Oman Based on a Multiscale and a Multidisciplinary Approach." *Hydrogeology Journal* 13, no. 5–6: 708–726. https://doi.org/10.1007/s10040-005-0449-2.

Dick, H. J. B., and T. Bullen. 1984. "Chromian Spinel as a Petrogenetic Indicator in Abyssal and Alpine-Type Peridotites and Spatially Associated Lavas." *Contributions to Mineralogy and Petrology* 86, no. 1: 54–76.

Dilek, Y., and H. Furnes. 2011. "Ophiolite Genesis and Global Tectonics: Geochemical and Tectonic Fingerprinting of Ancient Oceanic Lithosphere." *Bulletin* 123, no. 3–4: 387–411.

Dilek, Y., and H. Furnes. 2014. "Ophiolites and Their Origins." *Elements* 10, no. 2: 93–100. https://doi.org/10.2113/gselements.10.2.93.

Direction Interrégionale de Météo-France en Nouvelle-Calédonie et à Wallis-et-Futuna. 2022. "Climate Data From Noumea Station (988), 1991–2020." https://www.meteo.nc/.

Directorate General of Meteorology. 2020. *Ibra Station Climate Data (1986–2009)*. Public Authority for Civil Aviation. https://met.caa.gov.om/.

Ellis, G. S., and S. E. Gelman. 2024. "Model Predictions of Global Geologic Hydrogen Resources." *Science Advances* 10: eado0955. https://doi.org/10.1126/sciadv.ado0955.

Etiope, G. 2017. "Abiotic Methane in Continental Serpentinization Sites: An Overview." *Procedia Earth and Planetary Science* 17: 9–12. https://doi.org/10.1016/j.proeps.2016.12.006.

Etiope, G., and A. Ionescu. 2015. "Low Temperature Catalytic CO_2 Hydrogenation With Geological Quantities of Ruthenium: A Possible Abiotic CH_4 Source in Chromitite-Rich Serpentinized Rocks." *Geofluids* 15, no. 3: 438–452. https://doi.org/10.1111/gfl.12106.

Etiope, G., J. Judas, and M. J. Whiticar. 2015. "Occurrence of Abiotic Methane in the Eastern United Arab Emirates Ophiolite Aquifer." *Arabian Journal of Geosciences* 8, no. 12: 11345–11348. https://doi.org/10.1007/s12517-015-1975-4.

Etiope, G., and C. Oze. 2022. "Microbial vs Abiotic Origin of Methane in Continental Serpentinized Ultramafic Rocks: A Critical Review and the Need of a Holistic Approach." *Applied Geochemistry* 143: 105373. https://doi.org/10.1016/j.apgeochem.2022.105373.

Etiope, G., N. Samardžić, F. Grassa, H. Hrvatović, N. Miošić, and F. Skopljak. 2017. "Methane and Hydrogen in Hyperalkaline Groundwaters of the Serpentinized Dinaride Ophiolite Belt, Bosnia and Herzegovina." *Applied Geochemistry* 84: 286–296. https://doi.org/10.1016/j.apgeochem.2017.07.006.

Etiope, G., M. Schoell, and H. Hosgörmez. 2011. "Abiotic Methane Flux From the Chimaera Seep and Tekirova Ophiolites (Turkey): Understanding Gas Exhalation From Low Temperature Serpentinization and Implications for Mars." *Earth and Planetary Science Letters* 310, no. 1–2: 96–104. https://doi.org/10.1016/j.epsl.2011.08.001.

Etiope, G., and B. Sherwood Lollar. 2013. "Abiotic Methane on Earth." *Reviews of Geophysics* 51, no. 2: 276–299. https://doi.org/10.1002/rog.20011.

Etiope, G., B. Tsikouras, S. Kordella, E. Ifandi, D. Christodoulou, and G. Papatheodorou. 2013. "Methane Flux and Origin in the Othrys Ophiolite Hyperalkaline Springs, Greece." *Chemical Geology* 347: 161–174. https://doi.org/10.1016/j.chemgeo.2013.04.003.

Etiope, G., I. Vadillo, M. J. Whiticar, et al. 2016. "Abiotic Methane Seepage in the Ronda Peridotite Massif, Southern Spain." *Applied Geochemistry* 66: 101–113. https://doi.org/10.1016/j.apgeochem.2015.12.001.

Etiope, G., S. Vance, L. E. Christensen, J. M. Marques, and I. da Ribeiro Costa. 2013. "Methane in Serpentinized Ultramafic Rocks in Mainland Portugal." *Marine and Petroleum Geology* 45: 12–16. https://doi.org/10.1016/j.marpetgeo.2013.04.009.

Etiope, G., and M. J. Whiticar. 2019. "Abiotic Methane in Continental Ultramafic Rock Systems: Towards a Genetic Model." *Applied*

Geochemistry 102: 139–152. https://doi.org/10.1016/j.apgeochem.2019.01.012.

Evans, A. D., D. Craw, and D. A. H. Teagle. 2024. "Active Near-Surface Mobilisation of Slab-Derived Geochemical Signatures by Hyperalkaline Waters in Brecciated Serpentinites." *Chemical Geology* 643: 1–12. https://doi.org/10.1016/j.chemgeo.2023.121822.

Evans, A. D., D. A. H. Teagle, D. Craw, T. J. Henstock, and I. H. Falcon-Suarez. 2021. "Uplift and Exposure of Serpentinized Massifs: Modeling Differential Serpentinite Diapirism and Exhumation of the Troodos Mantle Sequence, Cyprus." *Journal of Geophysical Research: Solid Earth* 126, no. 6: 1–15. https://doi.org/10.1029/2020JB021079.

Evans, B. W., K. Hattori, and A. Baronnet. 2013. "Serpentinite: What, Why, Where?" *Elements* 9, no. 2: 99–106. https://doi.org/10.2113/gselements.9.2.99.

Federal Hydrometeorological Institute. 2001–2024. "Climate Data From Tuzla Station (1961–1990)." https://www.fhmzbih.gov.ba/latinica/.

Fones, E. M., D. R. Colman, E. A. Kraus, et al. 2019. "Physiological Adaptations to Serpentinization in the Samail Ophiolite, Oman." *ISME Journal* 13, no. 7: 1750–1762. https://doi.org/10.1038/s41396-019-0391-2.

Foustoukos, D. I., M. Bizimis, C. Frisby, and S. B. Shirey. 2015. "Redox Controls on Ni-Fe-PGE Mineralization and Re/Os Fractionation During Serpentinization of Abyssal Peridotite." *Geochimica et Cosmochimica Acta* 150: 11–25. https://doi.org/10.1016/j.gca.2014.11.025.

Frost, R. B., and J. S. Beard. 2007. "On Silica Activity and Serpentinization." *Journal of Petrology* 48, no. 7: 1351–1368. https://doi.org/10.1093/petrology/egm021.

Fujii, M., K. Okino, H. Sato, K. Nakamura, T. Sato, and T. Yamazaki. 2016. "Variation in Magnetic Properties of Serpentinized Peridotites Exposed on the Yokoniwa Rise, Central Indian Ridge: Insights Into the Role of Magnetite in Serpentinization." *Geochemistry, Geophysics, Geosystems* 17, no. 12: 5024–5035. https://doi.org/10.1002/2016GC006511.

Gass, I. G. 1980. "The Troodos Massif: Its Role in the Unravelling of the Ophiolite Problem and Its Significance in the Understanding of Constructive Plate Margin Processes."

Gazel, E., P. Denyer, and P. O. Baumgartner. 2006. "Geologica Acta: An International Earth Science Journal." *Costa Rica Geologica Acta: An International Earth Science Journal* 4, no. 2: 193–202.

Giampouras, M., C. J. Garrido, J. Zwicker, et al. 2019. "Geochemistry and Mineralogy of Serpentinization-Driven Hyperalkaline Springs in the Ronda Peridotites." *Lithos* 350: 350–351. https://doi.org/10.1016/j.lithos.2019.105215.

Giggenbach, W. F. 1975. "A simple method for the collection and analysis of volcanic gas samples." *Bulletin volcanologique* 39, no. 1: 132–145. https://doi.org/10.1007/BF025969.

Government of Newfoundland and Labrador. n.d. "Cow Point Station Climate Data (1983–2018)." https://www.gov.nl.ca/ecc/occ/climate-data/.

Holm, N. G., C. Oze, O. Mousis, J. H. Waite, and A. Guilbert-Lepoutre. 2015. "Serpentinization and the Formation of H_2 and CH_4 on Celestial Bodies (Planets, Moons, Comets)." *Astrobiology* 15, no. 7: 587–600. https://doi.org/10.1089/ast.2014.1188.

Hosgormez, H., G. Etiope, and M. N. Yalçin. 2008. "New Evidence for a Mixed Inorganic and Organic Origin of the Olympic Chimaera Fire (Turkey): A Large Onshore Seepage of Abiogenic Gas." *Geofluids* 8, no. 4: 263–273. https://doi.org/10.1111/j.1468-8123.2008.00226.x.

Hostetler, P. B., R. G. Coleman, F. A. Mumpton, and B. Evans. 1966. "Brucite in Alpine Serpentinites." *American Mineralogist* 51: 75–98.

Howells, A. E. G., J. A. M. Leong, T. Ely, et al. 2022. "Energetically Informed Niche Models of Hydrogenotrophs Detected in Sediments of Serpentinized Fluids of the Samail Ophiolite of Oman. Journal of Geophysical Research." *Biogeosciences* 127: e2021JG006317. https://doi.org/10.1029/2021JG006317.

Howells, A. E. G., K. Robinson, M. G. Silva, et al. 2025. "Methanotrophy Under Extreme Alkalinity in a Serpentinizing System." *bioRxiv*. https://doi.org/10.1101/2025.09.12.675893.

Hrachowitz, M., P. Benettin, B. M. van Breukelen, et al. 2016. "Transit Times—The Link Between Hydrology and Water Quality at the Catchment Scale." In *Wiley Interdisciplinary Reviews: Water*, vol. 3, 629–657. John Wiley and Sons Inc. https://doi.org/10.1002/wat2.1155.

Instituto Português do Mar e da Atmosfera. 2015. "Portalegre Station Climate Data (1971–2000)." *Programa ADAPT*. http://portaldoclima.pt/en/.

Iyer, K., H. Austrheim, T. John, and B. Jamtveit. 2008. "Serpentinization of the Oceanic Lithosphere and Some Geochemical Consequences: Constraints From the Leka Ophiolite Complex, Norway." *Chemical Geology* 249, no. 1–2: 66–90. https://doi.org/10.1016/j.chemgeo.2007.12.005.

Jackson, O., S. R. Lawrence, I. P. Hutchinson, A. E. Stocks, A. C. Barnicoat, and M. Poney. 2024. "Natural Hydrogen: Sources, Systems and Exploration Plays." *Geoenergy* 2, no. 1: geoenergy2024-002. https://doi.org/10.1144/geoenergy2024-002.

Josse, J., and F. Husson. 2016. "missMDA: A Package for Handling Missing Values in Multivariate Data Analysis." *Journal of Statistical Software* 70: 1–31. https://doi.org/10.18637/jss.v070.i01.

Kelemen, P. B., and C. E. Manning. 2015. "Reevaluating Carbon Fluxes in Subduction Zones, What Goes Down, Mostly Comes Up." *Proceedings of the National Academy of Sciences* 112, no. 30: E3997–E4006. https://doi.org/10.1073/pnas.1507889112.

Kelemen, P. B., J. Rg Matter, D. Walker, and L. Doherty. 2008. "In Situ Carbonation of Peridotite for CO_2 Storage." www.pnas.org/cgi/content/full/.

Kelemen, P. B., N. Shimizu, and V. J. M. Salters. 1995. "Extraction of Mid-Ocean-Ridge Basalt From the Upwelling Mantle by Focused Flow of Melt in Dunite Channels." *Nature* 375, no. 6534: 747–753.

Klein, F., W. Bach, S. E. Humphris, et al. 2014. "Magnetite in Seafloor Serpentinite—Some Like It Hot." *Geology* 42, no. 2: 135–138. https://doi.org/10.1130/G35068.1.

Klein, F., W. Bach, and T. M. McCollom. 2013. "Compositional Controls on Hydrogen Generation During Serpentinization of Ultramafic Rocks." *Lithos* 178: 55–69. https://doi.org/10.1016/j.lithos.2013.03.008.

Klein, F., and C. J. Garrido. 2011. "Thermodynamic Constraints on Mineral Carbonation of Serpentinized Peridotite." *Lithos* 126, no. 3–4: 147–160. https://doi.org/10.1016/j.lithos.2011.07.020.

Klein, F., N. G. Grozeva, and J. S. Seewald. 2019. "Abiotic Methane Synthesis and Serpentinization in Olivine-Hosted Fluid Inclusions." *Proceedings of the National Academy of Sciences of the United States of America* 116, no. 36: 17666–17672. https://doi.org/10.1073/pnas.1907871116.

Lamadrid, H. M., J. D. Rimstidt, E. M. Schwarzenbach, et al. 2017. "Effect of Water Activity on Rates of Serpentinization of Olivine." *Nature Communications* 8: 16107. https://doi.org/10.1038/ncomms16107.

Lê, S., J. Josse, A. Rennes, and F. Husson. 2008. "FactoMineR: An R Package for Multivariate Analysis." *Journal of Statistical Software* 25: 1–8. https://doi.org/10.18637/jss.v025.i01.

Leong, J. A., M. Nielsen, N. McQueen, et al. 2023. "H_2 and CH_4 Outgassing Rates in the Samail Ophiolite, Oman: Implications for Low Temperature, Continental Serpentinization Rates." *Geochimica et Cosmochimica Acta* 347: 1–15. https://doi.org/10.1016/j.gca.2023.02.008.

Leong, J. A. M., A. E. Howells, K. J. Robinson, et al. 2021. "Theoretical Predictions Versus Environmental Observations on Serpentinization Fluids: Lessons From the Samail Ophiolite in Oman." *Journal of Geophysical Research—Solid Earth* 126: e2020JB020756. https://doi.org/10.1029/2020JB020756.

Leong, J. A. M., and E. L. Shock. 2020. "Thermodynamic Constraints on the Geochemistry of Low Temperature, Continental, Serpentinization-Generated Fluids." *American Journal of Science* 320, no. 3: 185–235. https://doi.org/10.2475/03.2020.01.

Li Vigni, L., K. Daskalopoulou, S. Calabrese, F. Parello, and W. D'Alessandro. 2021. "Geochemical Characterisation of the Alkaline and Hyperalkaline Groundwater in the Othrys Ophiolite Massif, Central Greece." *Italian Journal of Geosciences* 141, no. 1: 42–56. https://doi.org/10.3301/ijg.2020.20.

Lollar, B. S., T. C. Onstott, G. Lacrampe-Couloume, and C. J. Ballentine. 2014. "The Contribution of the Precambrian Continental Lithosphere to Global H2 Production." *Nature* 516, no. 7531: 379–382. https://doi.org/10.1038/nature14017.

Marques, J. M., P. M. Carreira, M. R. Carvalho, et al. 2008. "Origins of High pH Mineral Waters From Ultramafic Rocks, Central Portugal." *Applied Geochemistry* 23, no. 12: 3278–3289. https://doi.org/10.1016/j.apgeochem.2008.06.029.

Marques, J. M., G. Etiope, M. O. Neves, et al. 2018. "Linking Serpentinization, Hyperalkaline Mineral Waters and Abiotic Methane Production in Continental Peridotites: An Integrated Hydrogeological-Bio-Geochemical Model From the Cabeço de Vide CH_4-Rich Aquifer (Portugal)." *Applied Geochemistry* 96: 287–301. https://doi.org/10.1016/j.apgeochem.2018.07.011.

Mayhew, L. E., E. T. Ellison, T. M. McCollom, T. P. Trainor, and A. S. Templeton. 2013. "Hydrogen Generation From Low Temperature Water-Rock Reactions." *Nature Geoscience* 6, no. 6: 478–484. https://doi.org/10.1038/ngeo1825.

McCollom, T. M., and W. Bach. 2009. "Thermodynamic Constraints on Hydrogen Generation During Serpentinization of Ultramafic Rocks." *Geochimica et Cosmochimica Acta* 73, no. 3: 856–875. https://doi.org/10.1016/j.gca.2008.10.032 Meteorological Service of New Zealand Ltd. (2008–2025). *Nelson Airport Station Observations (AWS-93546)*. https://www.metservice.com/.

McCollom, T. M., and J. S. Seewald. 2013. "Serpentinites, Hydrogen, and Life." *Elements* 9, no. 2: 129–134. https://doi.org/10.2113/gselements.9.2.129.

Meyer-Dombard, D. R., M. R. Osburn, D. Cardace, and C. A. Arcilla. 2019. "The Effect of a Tropical Climate on Available Nutrient Resources to Springs in Ophiolite-Hosted, Deep Biosphere Ecosystems in The Philippines." *Frontiers in Microbiology* 10: 761. https://doi.org/10.3389/fmicb.2019.00761.

Meyer-Dombard, D. R., K. M. Woycheese, E. N. Yargiçoğlu, et al. 2015. "High pH Microbial Ecosystems in a Newly Discovered, Ephemeral, Serpentinizing Fluid Seep at Yanartaş (Chimera), Turkey." *Frontiers in Microbiology* 5: 723. https://doi.org/10.3389/fmicb.2014.00723.

Miller, D. J., and N. I. Christensen. 1997. "Seismic Velocities of Lower Crustal and Upper Mantle Rocks From the Slow-Spreading Mid-AtlanticRidge, South of the Kane Fracture Transform Zone (MARK)." *Proceeding of the Ocean Drilling Program, Scientific Results* 153: 437–454. https://doi.org/10.2973/odp.proc.sr.153.043.1997.

Miller, H. M., J. M. Matter, P. Kelemen, et al. 2016. "Modern Water/Rock Reactions in Oman Hyperalkaline Peridotite Aquifers and Implications for Microbial Habitability." *Geochimica et Cosmochimica Acta* 179: 217–241. https://doi.org/10.1016/j.gca.2016.01.033.

Miyashiro, A. 1973. "The Troodos Ophiolitic Complex Was Probably Formed in an Island Arc." *Earth and Planetary Science Letters* 19, no. 2: 218–224.

Monnin, C., V. Chavagnac, C. Boulart, et al. 2014. "The Low Temperature Hyperalkaline Hydrothermal System of the Prony Bay (New Caledonia)." *Biogeosciences Discussions* 11: 6221–6267. https://doi.org/10.5194/bgd-11-6221-2014.

Monnin, C., M. Quéméneur, R. Price, et al. 2021. "The Chemistry of Hyperalkaline Springs in Serpentinizing Environments: 1. The Composition of Free Gases in New Caledonia Compared to Other Springs Worldwide." *Journal of Geophysical Research – Biogeosciences* 126, no. 9: 6243. https://doi.org/10.1029/2021JG006243.

Moores, E. M. 1982. "Origin and Emplacement of Ophiolites." *Reviews of Geophysics* 20, no. 4: 735–760.

Morrill, P. L., W. J. Brazelton, L. Kohl, et al. 2014. "Investigations of Potential Microbial Methanogenic and Carbon Monoxide Utilization Pathways in Ultra-Basic Reducing Springs Associated With Present-Day Continental Serpentinization: The Tablelands, NL, CAN." *Frontiers in Microbiology* 5: 613.

Müntener, O. 2010. "Serpentine and Serpentinization: A Link Between Planet Formation and Life." *Geology* 38, no. 10: 959–960. https://doi.org/10.1130/focus102010.1.

Neal, C., and P. Shand. 2002. "Spring and Surface Water Quality of the Cyprus Ophiolites." *Hydrology and Earth System Sciences* 6, no. 5: 797–817. https://doi.org/10.5194/hess-6-797-2002.

Neal, C., and G. Stanger. 1983. "Hydrogen Generation From Mantle Source Rocks in Oman." *Earth and Planetary Science Letters* 66: 315–320. https://doi.org/10.1016/0012-821x(83)90144-9.

Neal, C., and G. Stanger. 1985. "The Chemistry of Weathering."

Neubeck, A., L. Sun, B. Müller, et al. 2017. "Microbial Community Structure in a Serpentine-Hosted Abiotic Gas Seepage at the Chimaera Ophiolite, Turkey." *Applied and Environmental Microbiology* 83: 16. https://doi.org/10.1128/aem.03430-16.

Nothaft, D. B., A. S. Templeton, J. H. Rhim, et al. 2021. "Geochemical, Biological, and Clumped Isotopologue Evidence for Substantial Microbial Methane Production Under Carbon Limitation in Serpentinites of the Samail Ophiolite, Oman." *Journal of Geophysical Research – Biogeosciences* 126, no. 10: 6025. https://doi.org/10.1029/2020JG006025.

Ojeda, L., G. Etiope, P. Jiménez-Gavilán, et al. 2023. "Combining Methane Clumped and Bulk Isotopes, Temporal Variations in Molecular and Isotopic Composition, and Hydrochemical and Geological Proxies to Understand Methane's Origin in the Ronda Peridotite Massifs (Spain)." *Chemical Geology* 642: 121799. https://doi.org/10.1016/j.chemgeo.2023.121799.

Okland, I., S. Huang, H. Dahle, I. H. Thorseth, and R. B. Pedersen. 2012. "Low Temperature Alteration of Serpentinized Ultramafic Rock and Implications for Microbial Life." *Chemical Geology* 318–319: 75–87. https://doi.org/10.1016/j.chemgeo.2012.05.015.

Oufi, O., M. Cannat, and H. Horen. 2002. "Magnetic Properties of Variably Serpentinized Abyssal Peridotites." *Journal of Geophysical Research* 107, no. B5: 549. https://doi.org/10.1029/2001JB000549.

Pappalardo, L., G. Buono, M. Procesi, and G. Etiope. 2024. "The Link Between Ophiolitic Chromitites, Natural Hydrogen and Methane: Insights From 3D Microtomography." *Chemical Geology* 676: 122575. https://doi.org/10.1016/j.chemgeo.2024.122575.

Park, A. F. 1989. "Serpentinization." In *Petrology. Encyclopedia of Earth Science*. Springer. https://doi.org/10.1007/0-387-30845-8_221.

Paukert, A. N., J. M. Matter, P. B. Kelemen, E. L. Shock, and J. R. Havig. 2012. "Reaction Path Modeling of Enhanced In Situ CO_2 Mineralization for Carbon Sequestration in the Peridotite of the Samail Ophiolite, Sultanate of Oman." *Chemical Geology* 330: 86–100. https://doi.org/10.1016/j.chemgeo.2012.08.013.

Pawson, J. F. 2014. "Abiotic Methane Formation at the Dun Mountain Ophiolite, New Zealand."

Pearce, J. A., S. J. Lippard, and S. Roberts. 1984. "Characteristics and Tectonic Significance of Supra-Subduction Zone Ophiolites." *Geological Society, London, Special Publications* 16, no. 1: 77–94.

Peel, M. C., B. L. Finlayson, and T. A. McMahon. 2007. "Updated World Map of the Köppen-Geiger Climate Classification." *Hydrology and Earth System Sciences* 11: 1633–1644. https://doi.org/10.5194/hess-11-1633-2007.

Peters, E. K. 1993. "D-18O Enriched Waters of the Coast Range Mountains, Northern California: Connate and Ore Forming Fluids." *Geochimica et Cosmochimica Acta* 57: 1093–1104. https://doi.org/10.1016/0016-7037(93)90043-V.

Preiner, M., J. C. Xavier, F. L. Sousa, et al. 2018. "Serpentinization: Connecting Geochemistry, Ancient Metabolism and Industrial Hydrogenation." *Life* 8, no. 4: 41. https://doi.org/10.3390/life8040041.

Price, A. N., M. A. Zimmer, A. Bergstrom, et al. 2024. "Biogeochemical and Community Ecology Responses to the Wetting of Non-Perennial Streams." *Nature Water* 2, no. 9: 815–826. https://doi.org/10.1038/s44221-024-00298-3.

Proskurowski, G., M. D. Lilley, J. S. Seewald, et al. 2008. "Abiogenic Hydrocarbon Production at Lost City Hydrothermal Field." *Science* 319, no. 5863: 604–607. https://doi.org/10.1126/science.1151194.

Quéméneur, M., N. Mei, C. Monnin, et al. 2021. "Procaryotic Diversity and Hydrogenotrophic Methanogenesis in an Alkaline Spring (La Crouen, New Caledonia)." *Microorganisms* 9, no. 7: 1360. https://doi.org/10.3390/microorganisms9071360.

Quéméneur, M., N. Mei, C. Monnin, et al. 2023. "Microbial Taxa Related to Natural Hydrogen and Methane Emissions in Serpentinite-Hosted Hyperalkaline Springs of New Caledonia." *Frontiers in Microbiology* 14: 1196516. https://doi.org/10.3389/fmicb.2023.1196516.

Reeves, R. D., A. J. M. Baker, and R. Romero. 2007. "The Ultramafic Flora of the Santa Elena Peninsula, Costa Rica: A Biogeochemical Reconnaissance." *Journal of Geochemical Exploration* 93, no. 3: 153–159. https://doi.org/10.1016/j.gexplo.2007.04.002.

Rempfert, K. R., H. M. Miller, N. Bompard, et al. 2017. "Geological and Geochemical Controls on Subsurface Microbial Life in the Samail Ophiolite, Oman." *Frontiers in Microbiology* 8: 56. https://doi.org/10.3389/fmicb.2017.00056.

Republic of the Philippines, Department of Science and Technology, Philippine Atmospheric, Geophysical and Astronomical Services Administration, and Climatology and Agrometeorology Division. n.d. "Climate Data From Iba, Zambales Station (1991–2020)." https://www.pagasa.dost.gov.ph/.

Reynard, B., N. Hilairet, E. Balan, and M. Lazzeri. 2007. "Elasticity of Serpentines and Extensive Serpentinization in Subduction Zones." *Geophysical Research Letters* 34, no. 13: 176. https://doi.org/10.1029/2007GL030176.

Ross, C. M., B. Vega, L. Frouté, T.-W. Kim, and A. R. Kovscek. 2025. "Hydrogen Generation and Serpentinization of Olivine Under Flow Conditions." *Geophysical Research Letters* 52: e2024GL114016. https://doi.org/10.1029/2024GL114016.

Russell, M. J., A. J. Hall, and W. Martin. 2010. "Serpentinization as a Source of Energy at the Origin of Life." *Geobiology* 8, no. 5: 355–371. https://doi.org/10.1111/j.1472-4669.2010.00249.x.

Sabuda, M. C., W. J. Brazelton, L. I. Putman, et al. 2020. "A Dynamic Microbial Sulfur Cycle in a Serpentinizing Continental Ophiolite." *Environmental Microbiology* 22, no. 6: 2329–2345. https://doi.org/10.1111/1462-2920.15006.

Sader, J. A., M. I. Leybourne, M. B. McClenaghan, and S. M. Hamilton. 2007. "Low Temperature Serpentinization Processes and Kimberlite Groundwater Signatures in the Kirkland Lake and Lake Timiskiming Kimberlite Fields, Ontario, Canada: Implications for Diamond Exploration." *Geochemistry: Exploration, Environment, Analysis* 7, no. 1: 3–21. https://doi.org/10.1144/1467-7873/06-900.

Sánchez-Murillo, R., P. Gastezzi-Arias, R. Sánchez-Gutierrez, G. Esquivel-Hernandez, R. Perez-Salazar, and M. Poca. 2022. "Exploring Dissolved Organic Carbon Variations in a High Elevation Tropical Peatland Ecosystem: Cerro de la Muerte, Costa Rica." *Frontiers in Water* 3: 742780. https://doi.org/10.3389/frwa.2021.742780.

Sánchez-Murillo, R., E. Gazel, E. M. Schwarzenbach, et al. 2014. "Geochemical Evidence for Active Tropical Serpentinization in the Santa Elena Ophiolite, Costa Rica: An Analog of a Humid Early Earth?" *Geochemistry, Geophysics, Geosystems* 15, no. 5: 1783–1800. https://doi.org/10.1002/2013GC005213.

Sánchez-Murillo, R., L. G. Romero-Esquivel, J. Jiménez-Antillón, et al. 2019. "DOC Transport and Export in a Dynamic Tropical Catchment." *Journal of Geophysical Research: Biogeosciences* 124: 1665–1679. https://doi.org/10.15359/cicen.1.35.

Schrenk, M. O., W. J. Brazelton, and S. Q. Lang. 2013. "Serpentinization, Carbon, and Deep Life." *Reviews in Mineralogy and Geochemistry* 75: 575–606. https://doi.org/10.2138/rmg.2013.75.18.

Schulte, M., D. Blake, T. Hoehler, and T. McCollom. 2006. "Serpentinization and Its Implications for Life on the Early Earth and Mars." *Astrobiology* 6, no. 2: 364–376. https://doi.org/10.1089/ast.2006.6.36.

Schwander, L., M. Brabender, N. Mrnjavac, J. L. E. Wimmer, M. Preiner, and W. F. Martin. 2023. "Serpentinization as the Source of Energy, Electrons, Organics, Catalysts, Nutrients and pH Gradients for the Origin of LUCA and Life." *Frontiers in Microbiology* 14: 1257597. https://doi.org/10.3389/fmicb.2023.1257597.

Schwarzenbach, E. M., E. Gazel, and M. J. Caddick. 2014. "Hydrothermal Processes in Partially Serpentinized Peridotites From Costa Rica: Evidence From Native Copper and Complex Sulfide Assemblages." *Contributions to Mineralogy and Petrology* 168, no. 5: 1–21. https://doi.org/10.1007/s00410-014-1079-2.

Schwarzenbach, E. M., S. Q. Lang, G. L. Früh-Green, M. D. Lilley, S. M. Bernasconi, and S. Méhay. 2013. "Sources and Cycling of Carbon in Continental, Serpentinite-Hosted Alkaline Springs in the Voltri Massif, Italy." *Lithos* 177: 226–244. https://doi.org/10.1016/j.lithos.2013.07.009.

Searle, M., and J. Cox. 1999. "Tectonic Setting, Origin, and Obduction of the Oman Ophiolite." *GSA Bulletin* 111, no. 1: 104–122. https://doi.org/10.1130/0016-7606(1999)111%3C0104:TSOAOO%3E2.3.CO;2.

Seewald, J. S., M. Y. Zolotov, and T. McCollom. 2006. "Experimental Investigation of Single Carbon Compounds Under Hydrothermal Conditions." *Geochimica et Cosmochimica Acta* 70, no. 2: 446–460. https://doi.org/10.1016/j.gca.2005.09.002.

Sleep, N. H., A. Meibom, T. Fridriksson, R. G. Coleman, and D. K. Bird. 2004. "H_2-Rich Fluids From Serpentinization: Geochemical and Biotic Implications." *Proceedings of the National Academy of Sciences* 101: 12818–12823. https://doi.org/10.1073/pnas.0405289101.

Song, H., X. Ou, B. Han, et al. 2021. "An Overlooked Natural Hydrogen Evolution Pathway: Ni^{2+} Boosting H_2O Reduction by $Fe(OH)_2$ Oxidation During Low Temperature Serpentinization." *Angewandte Chemie International Edition* 60, no. 45: 24054–24058. https://doi.org/10.1002/anie.202110653.

Spahić, D., Z. Nikić, Z. M. Poznanović-Spahić, S. Mukherjee, and P. Dokmanović. 2023. "Discovery of Hyperalkaline Waters in the Ophiolites of Western Serbia: Environmental Considerations for Carbon Capture and Sequestration." *Geoenergy Science and Engineering* 231: 212319. https://doi.org/10.1016/j.geoen.2023.212319.

Stern, R. J. 2004. "Subduction Initiation: Spontaneous and Induced." *Earth and Planetary Science Letters* 226, no. 3–4: 275–292.

Suda, K., T. Aze, Y. Miyairi, et al. 2022. "The Origin of Methane in Serpentinite-Hosted Hyperalkaline Hot Spring at Hakuba Happo, Japan: Radiocarbon, Methane Isotopologue and Noble Gas Isotope

Approaches." *Earth and Planetary Science Letters* 585: 117510. https://doi.org/10.1016/j.epsl.2022.117510.

Suda, K., Y. Ueno, M. Yoshizaki, et al. 2014. "Origin of Methane in Serpentinite-Hosted Hydrothermal Systems: The CH_4-H_2-H_2O Hydrogen Isotope Systematics of the Hakuba Happo Hot Spring." *Earth and Planetary Science Letters* 386: 112–125. https://doi.org/10.1016/j.epsl.2013.11.001.

Suzuki, S., S. Ishii, A. Wu, et al. 2013. "Microbial Diversity in the Cedars, an Ultrabasic, Ultrareducing, and Low Salinity Serpentinizing Ecosystem." *Proceedings of the National Academy of Sciences of the United States of America* 110, no. 38: 15336–15341. https://doi.org/10.1073/pnas.1302426110.

Szponar, N., W. J. Brazelton, M. O. Schrenk, D. M. Bower, A. Steele, and P. L. Morrill. 2013. "Geochemistry of a Continental Site of Serpentinization, the Tablelands Ophiolite, Gros Morne National Park: A Mars Analogue." *Icarus* 224, no. 2: 286–296. https://doi.org/10.1016/j.icarus.2012.07.004.

Taran, Y., E. Kalacheva, D. Savelyev, B. Pokrovskii, and M. Bujakaite. 2024. "Hyperalkaline Waters and Travertines of the Ophiolite Complex of mt. Soldatskaya, Kamchatsky Mys Peninsula, Kamchatka, Russia." *Geochemical Journal* 58, no. 3: 127–137. https://doi.org/10.2343/geochemj.GJ24011.

Taran, Y. A., D. P. Savelyev, G. A. Pal'yanova, and B. G. Pokrovskii. 2023. "Alkali Waters of the Ultrabasic Massif of Mount Soldatskaya, Kamchatka: Chemical and Isotopic Compositions, Mineralogy, and 14C Age of Travertines." *Doklady Earth Sciences* 510: 262–268. https://doi.org/10.1134/S1028334X23600093.

Templeton, A. S., E. T. Ellison, C. Glombitza, et al. 2021. "Accessing the Subsurface Biosphere Within Rocks Undergoing Active Low-Temperature Serpentinization in the Samail Ophiolite (Oman Drilling Project)." *Journal of Geophysical Research – Biogeosciences* 126, no. 10: 6315. https://doi.org/10.1029/2021JG006315.

Templeton, A. S., E. T. Ellison, P. B. Kelemen, et al. 2024. "Low Temperature Hydrogen Production and Consumption in Partially-Hydrated Peridotites in Oman: Implications for Stimulated Geological Hydrogen Production." *Frontiers in Geochemistry* 2: 1–20. https://doi.org/10.3389/fgeoc.2024.1366268.

Thayer, T. P. 1966. "Serpentinization Considered as a Constant-Volume Metasomatic Process." *American Mineralogist* 51, no. 5–6: 685–710.

Tiago, I., and A. Veríssimo. 2013. "Microbial and Functional Diversity of a Subterrestrial High pH Groundwater Associated to Serpentinization." *Environmental Microbiology* 15, no. 6: 1687–1706. https://doi.org/10.1111/1462-2920.12034.

Ulrich, M., M. Muñoz, P. Boulvais, et al. 2020. "Serpentinization of New Caledonia Peridotites: From Depth to (Sub-)surface." *Contributions to Mineralogy and Petrology* 175, no. 9: 1–25. https://doi.org/10.1007/s00410-020-01713-0.

Vacquand, C., E. Deville, V. Beaumont, et al. 2018. "Reduced Gas Seepages in Ophiolitic Complexes: Evidences for Multiple Origins of the H2-CH4-N2 Gas Mixtures." *Geochimica et Cosmochimica Acta* 223: 437–461. https://doi.org/10.1016/j.gca.2017.12.018.

Vergara, M. T. G., V. A. M. Cabalo, and M. C. B. Arpa. 2023. "Geochemistry of Alkaline Springs and Ultramafic to Mafic Rocks in Botolan, Zambales: Significance to Carbon Sequestration." *International Multidisciplinary Scientific GeoConference Surveying Geology and Mining Ecology Management: SGEM* 23, no. 1.1: 33–41. https://doi.org/10.5593/sgem2023/1.1/s01.05.

Villalobos, R., and J. Retana. 2000. *Comparative Assessment of Agricultural Uses of ENSO Comparative Assessment of Agricultural Uses of ENSO-Based Climate Forecasts Costa Rica*. Instituto Meteorologico Nacional. https://www.researchgate.net/publication/301553150.

Villasante-Marcos, V., M. L. Osete, F. Gervilla, and V. García-Duenas. 2003. "Palaeomagnetic Study of the Ronda Peridotites (Betic Cordillera, Southern Spain)." *Tectonophysics* 377, no. 1–2: 119–141. https://doi.org/10.1016/j.tecto.2003.08.023.

Wang, Y., W. Li, B. J. Baker, et al. 2022. "Carbon Metabolism and Adaptation of Hyperalkaliphilic Microbes in Serpentinizing Spring of Manleluag, The Philippines." *Environmental Microbiology Reports* 14, no. 2: 308–319. https://doi.org/10.1111/1758-2229.13052.

Wantzen, K. M., C. M. Yule, J. M. Mathooko, and C. M. Pringle. 2008. "Organic Matter Processing in Tropical Streams." https://doi.org/10.1016/B978-012088449-0.50005-4.

Western Regional Climate Center. 2016–2025. "Ukiah, California (Station 049122) Climate Data (1893–2013)." https://wrcc.dri.edu/.

Whiticar, M. J. 1999. "Carbon and Hydrogen Isotope Systematics of Bacterial Formation and Oxidation of Methane." *Chemical Geology* 161: 291–314. https://doi.org/10.1016/S0009-2541(99)00092-3.

Wiebe, R., and L. Gaddy. 1934. "The Solubility of Hydrogen in Water at 0, 50, 75 and 100° From 25 to 1000 Atmospheres." *Journal of the American Chemical Society* 56, no. 1: 76–79. https://doi.org/10.1021/ja01316a022.

World Bank Group. 2025. "Climate Change Knowledge Portal." https://climateknowledgeportal.worldbank.org/.

World Meteorological Organization (WMO). 2024. "Climate Data." https://worldweather.wmo.int/en/home.html.

Worman, S. L., L. F. Pratson, J. A. Karson, and E. M. Klein. 2016. "Global Rate and Distribution of H2 Gas Produced by Serpentinization Within Oceanic Lithosphere." *Geophysical Research Letters* 43, no. 12: 6435–6443. https://doi.org/10.1002/2016GL069066.

Worman, S. L., L. F. Pratson, J. A. Karson, and W. H. Schlesinger. 2002. "Abiotic Hydrogen (H2) Sources and Sinks Near the Mid-Ocean Ridge (MOR) With Implications for the Subseafloor Biosphere." *Proceedings of the National Academy of Sciences* 117: 13283–13293. https://doi.org/10.1073/pnas.2002619117.

Yuce, G., F. Italiano, W. D'Alessandro, et al. 2014. "Origin and Interactions of Fluids Circulating Over the Amik Basin (Hatay, Turkey) and Relationships With the Hydrologic, Geologic and Tectonic Settings." *Chemical Geology* 388: 23–39. https://doi.org/10.1016/j.chemgeo.2014.09.006.

Zaccarini, F., G. Garuti, J. A. Proenza, et al. 2011. "Chromite and Platinum Group Elements Mineralization in the Santa Elena Ultramafic Nappe (Costa Rica): Geodynamic Implications." *Geologica Acta* 9, no. 3–4: 407–423. https://doi.org/10.1344/105.000001696.

Supporting Information

Additional supporting information can be found online in the Supporting Information section. **Figure S1:** Data coverage (%; log-scale) for each physico-chemical variable across 322 hyperalkaline samples. **Table S1:** Mean monthly precipitation (mm) and air temperature (°C) across continental serpentinization-influenced sites. **Table S2:** Physical and geochemical variables of low temperature continental serpentinization hyperalkaline sites. **Table S3:** Summary of Wilcoxon test statistics and significance Levels. **Data S1:** hyp70448-sup-0003-Supinfo.docx.